Journal Pre-proof

Migratory patterns and evolutionary plasticity of cranial neural crest cells in ray-finned fishes

Jan Stundl, Anna Pospisilova, Tereza Matějková, Martin Psenicka, Marianne E. Bronner, Robert Cerny

PII: S0012-1606(20)30228-1

DOI: https://doi.org/10.1016/j.ydbio.2020.08.007

Reference: YDBIO 8298

To appear in: *Developmental Biology*

Received Date: 27 April 2020

Revised Date: 13 August 2020

Accepted Date: 14 August 2020

Please cite this article as: Stundl, J., Pospisilova, A., Matějková, T., Psenicka, M., Bronner, M.E., Cerny, R., Migratory patterns and evolutionary plasticity of cranial neural crest cells in ray-finned fishes, *Developmental Biology* (2020), doi: https://doi.org/10.1016/j.ydbio.2020.08.007.

This is a PDF file of an article that has undergone enhancements after acceptance, such as the addition of a cover page and metadata, and formatting for readability, but it is not yet the definitive version of record. This version will undergo additional copyediting, typesetting and review before it is published in its final form, but we are providing this version to give early visibility of the article. Please note that, during the production process, errors may be discovered which could affect the content, and all legal disclaimers that apply to the journal pertain.

© 2020 Published by Elsevier Inc.

Journal Pre-proof

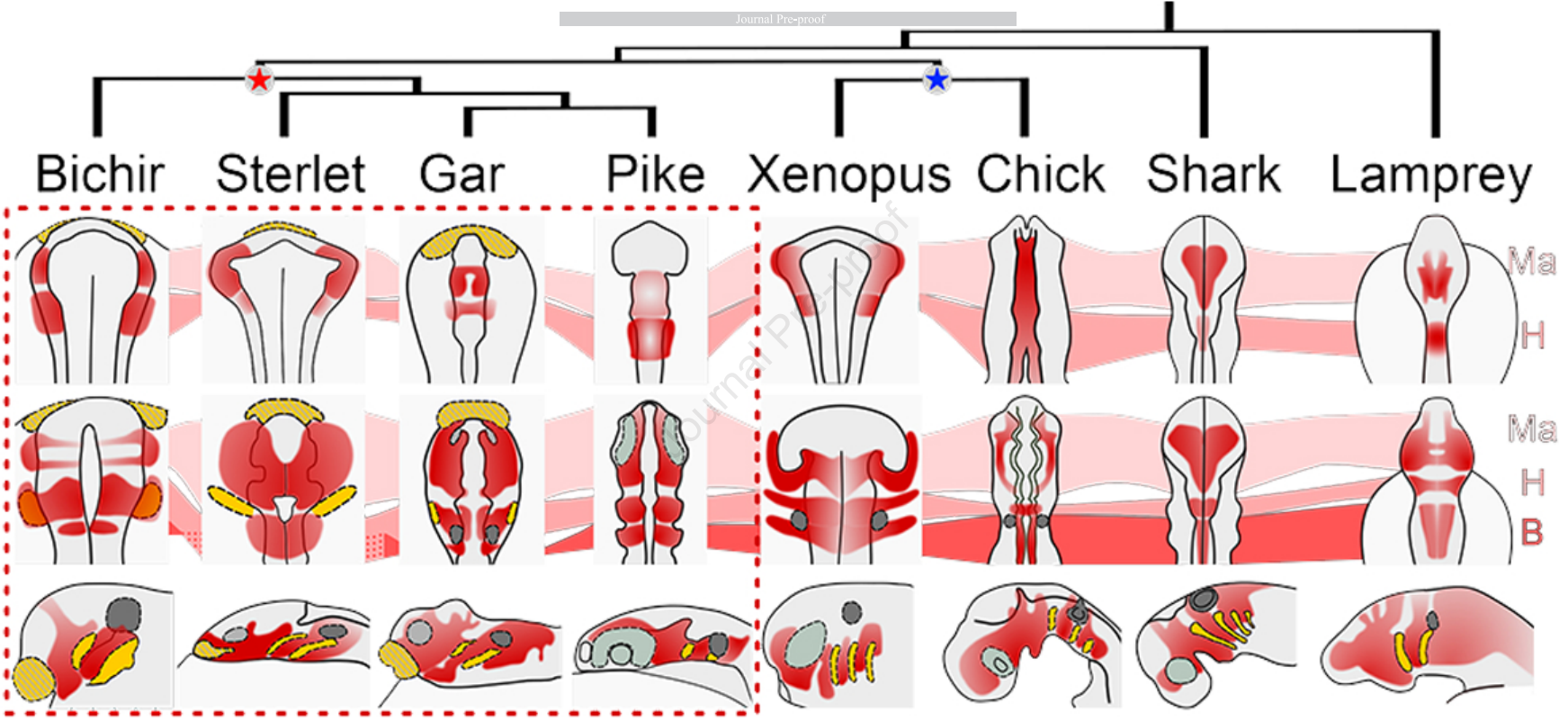

Journal Pre-proof

Migratory patterns and evolutionary plasticity of cranial neural crest cells in ray-finned fishes

Jan Stundl[a,b,c]*, Anna Pospisilova[a], Tereza Matějková[a], Martin Psenicka[c], Marianne E. Bronner[b], and Robert Cerny[a]*

[a]Department of Zoology, Faculty of Science, Charles University in Prague, Prague, Czech Republic

[b]Division of Biology and Biological Engineering, California Institute of Technology, Pasadena, CA, USA

[c]South Bohemian Research Center of Aquaculture and Biodiversity of Hydrocenoses, Faculty of Fisheries and Protection of Waters, University of South Bohemia in Ceske Budejovice, Vodnany, Czech Republic

* Correspondence to: Dr. Jan Stundl jstundl@caltech.edu

Dr. Robert Cerny robert.cerny@natur.cuni.cz

Journal Pre-proof

Journal Pre-proof

Abstract

The cranial neural crest (CNC) arises within the developing central nervous system, but then migrates away from the neural tube in three consecutive streams termed mandibular, hyoid and branchial, respectively, according to the order along the anteroposterior axis. While the process of neural crest emigration generally follows a conserved anterior to posterior sequence across vertebrates, we find that ray-finned fishes (bichir, sterlet, gar, and pike) exhibit several heterochronies in the timing and order of CNC emergence that influences their subsequent migratory patterns. First, emigration of the cranial neural crest in these fishes occurs prematurely compared to other vertebrates, already initiating during early neurulation and well before neural tube closure. Second, delamination of the hyoid stream occurs prior to the more anterior mandibular stream; this is associated with early morphogenesis of key hyoid structures like external gills (bichir), a large opercular flap (gar) or first forming cartilage (pike). In sterlet, the hyoid and branchial CNC cells form a single hyobranchial sheet, which later segregates in concert with second pharyngeal pouch morphogenesis. Taken together, the results show that despite generally conserved migratory patterns, heterochronic alterations in the timing of emigration and pattern of migration of CNC cells accompanies morphological diversity of ray-finned fishes.

Keywords: neural crest, vertebrates, craniofacial, evolution, neurulation

Journal Pre-proof

Introduction

Evolution of vertebrates is intimately connected with the advent of the neural crest (Gans and Northcutt, 1983; Northcutt and Gans, 1983; Northcutt, 2005; Green et al., 2015). This embryonic cell population arises within the forming neural tube but then migrates into the periphery to contribute to a remarkable range of structures and cell types such as odontoblasts, facial bone and cartilage, pigment cells, glial cells of the peripheral nervous system, components of heart, etc. (Bronner and Le Douarin, 2012; Simoes-Costa and Bronner, 2015; Hall, 2009; Le Douarin and Dupin, 2014). Given its contribution to a plethora of cell types, acquisition of this vertebrate-specific cell types was a key milestone in the evolutionary success of vertebrates on Earth (Gans and Northcutt, 1983; Forey and Janvier, 1994; Donoghue and Keating, 2014; Square et al., 2017).

The vertebrate neural crest is characterized by three key features: (i) multipotency, (ii) origin from the neural plate border, and (iii) ability to migrate long-distance in a directed fashion to diverse locations throughout the embryo (Theveneau and Mayor, 2012; Meulemans Medeiros, 2013; Green et al., 2015). Induction of the neural crest initiates already during gastrulation (Basch et al., 2006; Patthey et al., 2008; Betters et al., 2018). Following neurulation, individual neural crest (NC) cells begin to emigrate from the neural tube via an epithelial to mesenchymal transition controlled by interactions between transcriptional regulators, receptors, and signaling molecules (Sauka-Spengler and Bronner-Fraser, 2008; Simoes-Costa et al., 2014; Hockman et al., 2019). While NC cells arise all along the anteroposterior axis of the embryo, they follow different migratory pathways and form different derivatives depending upon their axial level of origin (Kuo and Erickson, 2010; Simoes-Costa and Bronner, 2013; Simoes-Costa and Bronner, 2015; Gouignard et al., 2018; Rothstein et al., 2018).

The most anterior and diverse neural crest population is the cranial neural crest (CNC), which migrates in three wide streams called the mandibular, hyoid and branchial, each

Journal Pre-proof

separated by neural crest-free zones adjacent to rhombomere 3 and 5 (Kulesa et al., 2010; Theveneau and Mayor, 2012; Szabó and Mayor, 2018). This migratory pattern of CNC cells appears to be mostly conserved across all vertebrates (Falck et al., 2002; Minoux and Rijli, 2010; Theveneau and Mayor, 2012; Rocha et al., 2019).

During migration, CNC cells interact not only with each other within individual streams but also with surrounding tissues (Carmona-Fontaine et al., 2008; Kulesa et al., 2010; Szabó and Mayor, 2018). One key interacting tissue is the head endoderm of the pharyngeal pouches (Graham, 2008; Grevellec and Tucker, 2010). In the final phase of migration, the endoderm influences CNC differentiation into cartilage precursors (Piotrowski and Nüsslein-Volhard, 2000; David et al., 2002; Crump et al., 2004). Thus, modulations of the head endoderm, and heterochronic and heterotopic alterations of CNC migratory patterns might represent a key source of craniofacial diversity in vertebrates (Schneider, 2018).

To better understand the diversity in patterns of CNC migration, it is essential to compare diverse species. To this end, here we investigate CNC cells in representatives of each phylogenetic lineage of non-teleost ray-finned fishes: bichir, sterlet, and gar (Betancur-R et al., 2017; Hughes et al., 2018; Kunz et al., 2009). All these species reflect evolutionarily informative lineages of ray-finned fishes. These species were chosen because they possess characteristics that either resemble lungfishes, amphibians or are transitional between amphibian-like and teleost-like (Cooper and Virta, 2007; Soukup et al., 2013; Minarik et al., 2017; Stundl et al., 2019). For comparison, we also investigate CNC cells of the northern pike as a representative of teleosts. Close examination of early CNC development in these species holds the promise of shedding light on craniofacial evolution of vertebrates, since all these ray-finned fishes possess distinct craniofacial characteristics, such as a massive exoskeleton in bichir, a distinct rostrum in sterlet, and significantly elongated jaws in gar and pike. The results reveal surprising alterations in CNC migration in all species and demonstrate that the migratory patterns of CNC cells are

not as stereotypic as generally assumed. This highlights the plasticity of CNC, which apparently contributes to remarkable craniofacial diversity across vertebrates.

Materials and methods

Fish embryo collections and histology

This study was performed by analysis of detailed developmental series of the Senegal bichir (*Polypterus senegalus* Cuvier, 1829), the sterlet sturgeon (*Acipenser ruthenus* Linnaeus, 1758), the tropical gar (*Atractosteus tropicus* T. N. Gill, 1863) and the northern pike (*Esox lucius* Linnaeus, 1758). Husbandry and collection of embryos were performed as previously described (Minarik et al., 2017; Pospisilova et al., 2019), with embryos being staged as previously described (Dettlaff et al., 1993; Long and Ballard, 2001; Diedhiou and Bartsch, 2009; Pospisilova et al., 2019), fixed in 4% paraformaldehyde (PFA) in 0.1 M PBS at 4°C overnight, and dehydrated in 100% methanol for storage at -20°C. This study was conducted by following institutional guidelines for the use of embryonic material and international animal welfare guidelines (Directive 2010/63/EU) in the animal facility of the Department of Zoology, Charles University in Prague. As the use of standard staging tables is unsuitable for direct interspecies comparison, we instead utilize four developmental stages: specification, emigration, early and late migration (Fig. 3-6). To this end, we first analyzed each described developmental stage relevant to the neural crest migration (from late gastrula until pharyngula stage) and based on the obtained data we designated individual stages as follows: specification – first detected expression of neural crest markers; emigration - the developmental stage when one of the neural crest streams begins emigration from the prospective neural tube; early migration - post-neurula stage or early pharyngula stage containing migratory CNC cells; late migration - pharyngula stage with fully developed pharyngeal pouches.

Journal Pre-proof

Embryos for histological analyses were embedded in JB4 resin (Polysciences) according to the manufacturer's instructions, sectioned on RM2155 microtome (Leica, Germany) to 4 µm-thick sections, stained with Azure B-Eosin (SERVA), mounted in DePeX (SERVA), and photographed using microscope BX51 (Olympus, Japan). Cartilage staining was performed with Alcian Blue as described previously (Taylor and Van Dyke, 1985), and photographed using a dissection microscope SZX12 (Olympus, Japan).

Scanning electron microscopy and micro-CT imaging and analysis

Specimens for scanning electron microscopy (SEM) and micro-CT were fixed in 4% PFA in 0.1 M PBS and transferred into modified Karnovsky fixative (Mitgutsch et al., 2008) at least overnight. Samples for SEM were washed in PBS, dehydrated through a graded series of ethanol, transferred into dehydrating capsules with 30µm pores (SPI Supplies, Germany), and dried in a critical point dryer CPD 030 (BAL-TEC, Liechtenstein). Dried samples were mounted on a steel disc covered by Tempfix resin (SPI Supplies, Germany), and coated with gold in SCD 050 sputter coater (BAL-TEC, Liechtenstein). SEM images were obtained using a JSM-6380LV scanning electron microscope (JEOL, Japan). Specimens for micro-CT visualization were prepared as described previously (Metscher, 2009; Minarik et al., 2017) and scanned with a MicroXCT-200 (Zeiss/Xradia, Germany) at the Department of Theoretical Biology, University of Vienna and with a SkyScan 1172 (Bruker, USA) at the Paleontological Department of the National Museum, Prague. Tomographic sections were reconstructed in XMReconstructor (Zeiss/Xradia, Germany), and final visualizations were accomplished in AMIRA 6.0.1 (Thermo Fisher Scientific, USA). The original microCT scans were uploaded to the Morphobank (http://morphobank.org/permalink/?P3784).

Journal Pre-proof

Probes synthesis and in situ hybridization

Primers for PCR amplification were designed based on sequences from *de novo* assembled transcriptomes of non-teleost fishes and on predicted gene sequences in the northern pike genome assembly (Rondeau et al., 2014). Probe templates were isolated by direct amplification from cDNA libraries using specific primers (Table 1), cloned into pGEM-T Easy Vector (Promega), and sequenced.

Table 1. *List of primer sequences used for probe synthesis.*

Gene	Forward primer	Reverse primer
*Hand2*_At	5'-ATHAGCCAYCCAGAGATGTC-3'	5'- TTTGAATTCCGCTTTGAAGG -3'
*Hand2*_El	5'- CTTACCTYATGGACATTCTG -3'	5'- CAAATATCCAMTSTCCGTAG -3'
*Hand2*_Ps	5'- CAGGACTCAGAGCATCAACAG -3'	5'- CTTTRGTTTTGTCRTTGCTGC -3'
*FoxD3*_Ar	5'- GAYGTGGAYATCGAYGTGGT -3'	5'- CTSARRAARCTVCCGTTGTC -3'
*FoxD3*_At	5'- ARYAAGCCHAAAAACAGCCT -3'	5'- TCGAACATRTCTTCDGACTG -3'
*FoxD3*_El	5'- GAYGTGGAYATCCGAYGTGGT -3'	5'- CTSARRAARCTVCCGTTGTC -3'
Hoxa2_Ps	5'- CTGTCGGTGATDCATTTCAAAG -3'	5'- ARCTYTGGGAHTCDCYATTG -3'
Krox20_Ar	5'- CAGACTTTCACCTACATGGG -3'	5'- ATRTGBGTGGTRAGGTGGTC -3'
Krox20_At	5'- CAGACTTTCACCTACATGGG -3'	5'- ATRTGBGTGGTRAGGTGGTC -3'
Krox20_El	5'- TTTCCCATCATCCCGGACTA -3'	5'- ATGTGTCTGGTTAGCTCGTC -3'
Krox20_Ps	5'- ATGGTCAATGTGGATATGAG -3'	5'- AGGGCATGGAAAGGGCTTGC -3'
Snail1/2_Ps	5'- TACAGCGAACTGGAAAGCCA -3'	5'- GAGCGGATGTGCATYTTCAG -3'
Sox9_Ar	5'- GGCAGAACGAAGCTGAAGAC -3'	5'- CATACTGGGAGCGTGTGATG -3'
Sox9_At	5'- CCAGTACCCTCACCTTCACA -3'	5'- ATGACATCGCTGCTCAGCTC -3'

Sox9_El	5'- TTCAAGCTTTTCCACGTGCG -3'	5'- ATCGTAGCCCTTCAGGACCT -3'
Sox9_Ps	5'- CTCMGCTGCTCCGTYTTDATSTG -3'	5'-TGGWSYYTGGTGCCBATGCCNGT -3'
Sox10_Ar	5'- GAKTACAAGTACCAGCCCNCG -3'	5'- GGNAGGTACTGGTCRAAYTC -3'
Sox10_At	5'- CTGTGGAGGCTTCTGAACGGA -3'	5'- GTGCAKGCTCTTGTAGTGCG -3'
Sox10_El	5'- TACAAGTACCAGCCACGYMG -3'	5'- GGNAGGTACTGGTCRAAYTC -3'
Twist1_Ar	5'- GAAAWGWTGCARGANGAATC -3'	5'- TGVGATGYRGACATGGCCA -3'

Digoxygenin-labeled probes were prepared by standard protocols. Whole mount in situ hybridization was performed as described previously (Minarik et al., 2017). Selected embryos were washed in 0.1M PBS, transferred into the embedding medium (gelatin, albumin, and glutaraldehyde), and sectioned on VT1200S vibratome (Leica, Germany) at 50 µm-thickness. For better visualization of tissue context, the sections were counterstained with Fluoroshield with DAPI (Sigma), and photographed using a BX51 (Olympus, Japan) fluorescent microscope.

Antibody staining and fate-mapping analysis

Embryos for antibody staining were transferred from 100% methanol into Dent's fixative (80% methanol and 20% DMSO) for six hours, washed three times in PBST (0.1M PBS and 0.4% Triton X-100), and then incubated in Antibody diluent buffer (DAKO) for one hour. Subsequently, primary antibody was applied overnight at room temperature in a damp box. After incubation, the embryos were washed three times in PBST, transferred in Antibody diluent buffer, and incubated with the secondary antibody in a damp box at room temperature for 5-6 hours. After labeling, the specimens were washed in 0.1M PBS and transferred to clearing solution (benzyl alcohol/benzyl benzoate; 2:1). Neural crest cells were labeled with Sox9 antibody (AB5535;

Merck Millipore), and primary antibody was detected by Alexa Fluor 594 (Invitrogen, Thermo Fisher Scientific Inc.). For the fate-mapping analysis, individual embryos were decapsulated and mounted into a Petri dish with plasticine, which helped to orient the embryo before injection. CM-DiI cell tracking dye (Thermo Fisher Scientific Inc.) was prepared for injection as described (Minarik et al., 2017). CM-DiI was injected through the inner egg membrane into the region of prospective CNC. All injected embryos were allowed to develop until the desired stage when the embryos were euthanized with an overdose of MS-222 (Sigma) and fixed in 4% PFA in 0.1M PBS. For visualization of early neurula stages of pike, embryos were dechorionated and stained with DAPI. Images were taken using Lumar V.12 (Zeiss, Germany).

Results

Transitional patterns of neurulation

The central nervous system of all vertebrates arises during neurulation which occurs by two distinct mechanisms depending on species: (i) invagination of the neural plate until the neural folds meet to form the neural tube (primary neurulation best studied in amniotes) or (ii) cavitation of the neural keel (best studied in teleosts) (Baker and Bronner-Fraser, 1997; Lowery and Sive, 2004; Harrington et al., 2009). We first analyzed the external morphology of cranial neurulation in individual non-teleost fish lineages. SEM images reveal variation in the mechanism of cranial neurulation across species examined here (Fig. 1). Bichir and sterlet embryos undergo primary neurulation with lateral regions of the neural plate forming neural folds, which then roll up and bend into a neural tube with a central lumen (Fig. 1A-H). Nevertheless, both species exhibit remarkable differences in neurulation. In bichir, the entire morphogenetic process occurs above the yolk ball (Fig. 1A-D). In contrast, in sterlet, formation of the neural tube takes place within the yolk ball (Fig. 1E-H), and the developing neural tube is

not as elevated as in bichir (cf. Fig. 1D, H). Gar embryos undergo neurulation in a manner that is similar that described for teleosts including pike (Schmitz et al., 1993; Lowery and Sive, 2004; Pospisilova et al., 2019) with the neuroectoderm forming a solid neural keel that only later develops a central lumen of the neural tube by means of cavitation (Fig. 1I-L).

Taken together, non-teleost fish embryos seem to manifest transitional patterns from primary neurulation to neurulation via cavitation, depending on the species. Interestingly, such transitional patterns are also apparent in gastrulation of non-teleost fishes (Takeuchi et al., 2009).

Accelerated emigration of cranial neural crest cells

In vertebrates, CNC cells typically begin their migration around the time of or after neural tube closure (Tan and Morris-Kay, 1986; Noden, 1988; Horigome et al., 1999; Smith, 2001; Falck et al., 2002; Mitgutsch et al., 2008; Diaz et al., 2019). To characterize the onset of CNC cells emigration, we screened for spatiotemporal expression of *Sox9*, a member of the SoxE transcription factor family, which is expressed in premigratory and migratory neural crest cells and later is associated with chondrogenesis (Cheung and Briscoe, 2003; Mori-Akiyama et al., 2003; Martik and Bronner, 2017). Embryos were examined at two stages: onset of migration and mid-migratory phase (Fig. 2).

In all studied fish species, the first migrating CNC cells are already detectable during the first phase of neurulation. In bichir and sterlet, this occurs before neural tube closure, whereas in gar and pike before lumen formation (Fig. 2). In bichir, *Sox9* expression is apparent in both the mandibular and hyoid regions, even when the neural tube is still widely open (Fig. 2A). However, histological sections reveal that there is a difference between the mandibular and hyoid regions (Fig. 2B-C'; Stundl et al., 2019); whereas *Sox9* is detected in premigratory cells in

the mandibular region (Fig. 2B-B'), it is strongly expressed in already emigrating cells of the hyoid stream (Fig. 2C-C'). At a later stage, when the neural tube is still open, *Sox9* transcripts are more abundant in the hyoid region than in the mandibular region (Fig. 2D), and the hyoid neural crest stream is predominant (Fig. 2D-F'). In sterlet, the mandibular region has strong *Sox9* expression compared to the hyoid region (Fig. 2G). Transverse sections reveal *Sox9* transcripts in emigrating cells of the mandibular neural crest stream (Fig. 2H-H') and presumptive CNC cells of the hyoid stream (Fig. 2I-I'). At later stages of neurulation, *Sox9* transcripts are seen in migrating cells of the mandibular stream and in emigrating cells of the hyoid stream (Fig. 2J-L'). As neurulation begins in gar, *Sox9* is detected only in presumptive CNC in the mandibular region (Fig. 2M-O'). Interestingly, at later stages, *Sox9* expression is detected in the emigrating hyoid NC cells contrasting with the mandibular NC cells, which still reside within the neural plate border (Fig. 2P-R'). In pike, the first *Sox9* transcripts are detectable concomitantly in mandibular and hyoid CNC, but the expression is again more intense in the hyoid region (Fig. 2S). Transverse sections at this early stage show *Sox9* positive cells in the neuroepithelium of the neural plate border in the mandibular region, while sections of the hyoid region reveal strong expression in already migrating CNC cells (Fig. 2S-U'). At later stages of neurulation, CNC cells maintain strong *Sox9* expression particularly in the hyoid stream (Fig. 2V-X').

This comparative analysis of spatiotemporal *Sox9* expression demonstrates that in bichir, gar, and pike, the hyoid CNC cells are uniquely accelerated in their migration compared to the mandibular CNC cells (cf. Fig. 2A-C'; P-R'; S-U'). In contrast, CNC cells in sterlet embryos follow the canonical sequential anteroposterior order in emigration (Fig. 2G-L').

Cranial neural crest cells patterning and migration

Journal Pre-proof

Having established patterns of premigratory and migratory neural crest cells, we sought to examine spatiotemporal changes in the expression of Sox9 and other neural crest genes at multiple stages. To this end, we identified four critical stages of neural crest development: (i) specification, (ii) emigration, (iii) early phase and (iv) late phase of migration (Fig. 3-6). We examined the expression of several neural crest specifier genes: *Sox9*, *Sox10*, *FoxD3*, *Snail1/2* and *Twist1*, together with *Krox20,* a marker for rhombomeres 3 (r3) and 5 (r5) which separates individual neural crest streams (Fig. 3-6) (Wilkinson et al., 1989; Nieto et al., 1995; Sauka-Spengler and Bronner-Fraser, 2008; Simoes-Costa and Bronner, 2015; Martik and Bronner, 2017). For better resolution, we also analyzed SOX9 protein expression in all examined species, from emigration through the late phase of migration (Fig. 7).

In bichir, *Sox9,* and *FoxD3* genes are the earliest neural crest specifier genes expressed in the presumptive mandibular and hyoid neural crest streams (Fig. 3I, Q) and their expressions persists through later stages (Fig. 3J-L, R). Although *Sox9* expression overlaps with that of *FoxD3* during early neurulation, the *FoxD3* signal is weaker than *Sox9* (cf. Fig. 3I-J and Fig. 3Q-R). During the emigration phase, in the mandibular region, Sox9 expression resolves into two distinct stripes corresponding to the presumptive subpopulations of the mandibular stream (Fig. 3J; Fig. 7A; Fig. S1). In more posterior regions of the developing head, *Sox9* is strongly expressed in the migrating cells of the hyoid CNC and is first seen in cells of the branchial streams (Fig. 3J; Fig. 7A). During the migratory phase, *Sox9* and *Snail1/2* expressions are predominantly located in the hyoid region (Fig. 3K, P). SOX9 immunostaining yielded similar results (Fig. 7B). A few *Snail1/2*-positive and SOX9-positive migratory mandibular CNC cells were also observed in close contact with the pre-oral gut (Fig. 3P; Fig. 7C), which represents the rostral-most endodermal head domain (Minarik et al., 2017).

In sterlet, we examined several neural crest genes such as *Sox9*, *Sox10*, *FoxD3*, and *Twist1* (Fig. 4). At the early neurula stage, while *Sox9* and *FoxD3* transcripts are detected in

Journal Pre-proof

prospective mandibular and hyoid CNC cells, *Sox10* is detected only in mandibular CNC cells, and *Twist1* is not detected in CNC at this stage (Fig. 4I, M, Q, U). During emigration, *Sox9*/SOX9-positive and *FoxD3*-positive cells are observed in the emigrating CNC of the mandibular and hyoid streams (Fig. 4J, R; Fig. 7D), and expression can also be seen in newly emigrating branchial CNC posterior to r5 (cf. Fig. 4F and Fig. 4J, R). At this developmental stage, *Sox10* and *Twist1* transcripts are detectable only in the mandibular CNC (Fig. 4N, V). During early migration, mandibular CNC marked by *Sox9*, *Sox10*, *FoxD3*, *Twist1* and also by SOX9 antibody comprises the vast majority of neural crest cells in the developing head (Fig. 4K, O, S, W; Fig. 7E). Interestingly, our data show that the hyoid and branchial neural crest migrate as a single sheet of cells from the level of hindbrain into the presumptive pharyngeal region, thus forming a common 'hyobranchial sheet' (Fig. 4O, K, S; Fig. S2). We also observed distinct stripes of *Krox20* expression lateral to the neural tube at the level of r5, which co-localized with *Twist1* (Fig. 4G, W), corresponding to the cells of the cardiac neural crest (Odelin et al., 2018). Next, we examined the later phase of CNC cell migration. While *Sox9* and *Twist1* are expressed in the majority of CNC cells, *Sox10* and *FoxD3* transcripts are found in cells of the hyoid and branchial neural crest streams and in a small number of mandibular CNC cells (Fig. 4L, P, T, X). In the mandibular region, *Sox9* and *Twist1* were expressed in two distinct subpopulations, the mandibular and maxillary branches (Fig. 4L, X; Cerny et al., 2004). Furthermore, our data show that cells of the mandibular neural crest stream migrate around the pre-oral gut, similar to that observed in bichir embryos (cf. Fig. 4K-L, O, W-X; Fig. 7F and Fig. 3P; Fig. 7C). At this stage, the hyobranchial sheet is completely divided into hyoid and branchial streams (cf. Fig. 4O, P and Fig. 7F).

At the beginning of gar neurulation, neural crest specifiers are first seen in cells of the prospective mandibular neural crest stream (Fig. 5I, M, Q). While *Sox9* is strongly expressed in CNC located in the dorsal and lateral part of the forming neural tube, *FoxD3* and *Sox10* are

Journal Pre-proof

expressed in cells lateral to the neural tube (Fig. 5I, M, Q). In slightly older embryos during emigration, CNC cells marked by *Sox9*/SOX9, *FoxD3,* and *Sox10* can be seen in the mandibular and hyoid regions (Fig. 5J, N, R; Fig. 7G), but emerging CNC cells are detectable only in the hyoid region (see Fig. 2). During early migration, expression of *Sox9* and *Sox10* can be seen in freshly emigrating mandibular and migrating CNC cells (Fig. 5K, S). By immunostaining, we identified SOX9+ cells of the branchial neural crest stream (Fig. 7H). At late migration, *Sox9* transcripts are detected throughout the otic vesicle (Fig. 5L), but the *FoxD3* signal is no longer detected at this stage (Fig. 5P). In gar, similar to sterlet embryos, *Krox20* expression is also detectable in cardiac neural crest cells (Fig. 5H). SOX9 immunostaining marks the whole CNC population at the late phase of migration, including two segregated branchial neural crest streams (Fig, 7I). Furthermore, *Sox10* expression is maintained in migrating mandibular and hyoid CNC cells (Fig. 5T). As in bichir and sterlet embryos, we also observed a similar migratory pattern of mandibular CNC cells migrating in close contact with the pre-oral gut in gar embryos (Fig. 5T; Fig. 7H, I)

Next, we characterized the expression of neural crest markers across developmental time-course in pike (Fig. 6A-D). During the specification stage, mandibular and hyoid CNC cells are marked by *Sox9* expression *(*Fig. 6I). A small number of *Sox9*-positive cells are located lateral to the forming neural tube, while a large number of *Sox9*/SOX9-positive cells are found in the dorsal neural tube spreading more into the hyoid region (Fig. 6I; Fig. 7J). At later developmental stages, *Sox9/*SOX9-positive cells are maintained in migratory mandibular and hyoid CNC cells and are detected for the first time in branchial neural crest (Fig. 6J; Fig. 7K). We also observed an overlap between *Sox10* and *FoxD3* expressions in CNC cells in the dorsal aspect of the neural tube (Fig. 6M, P). At the migratory phase, *Sox9, FoxD3,* and *Sox10* expression mark the maxillo-mandibular and preoptic subpopulation of the mandibular neural

Journal Pre-proof

crest (Fig. 6K-L, N-O, Q-R). At this stage, distinct hyoid and branchial neural crest streams can be resolved (Fig. 6K-L, N-O, Q-R; Fig. 7L).

Accelerated hyoid neural crest stream is associated with different hyoid structures in different species

Previous observations reveal remarkably accelerated development of the hyoid neural crest in bichir, gar, and pike embryos (Fig. 8A-D, F-I, K-N). We thus asked if the accelerated formation of the hyoid neural crest is correlated with advanced morphogenesis of species-specific hyoid structures. To examine this possibility, we utilized *Hand2* expression, which marks the ventralmost CNC cells in the developing pharyngeal arches (Cerny et al., 2010; Compagnucci et al., 2013; Square et al., 2015) and thus reveals the first CNC cells populating the pharyngeal region. In bichir, the first *Hand2*-positive cells are observed in the developing hyoid external gills, which form prominent head larval structures (cf. Fig. 8D and Fig. 8E). Similarly, in gar embryos, *Hand2* expression is first detectable in the hyoid region (Fig. 8I), correlating with the early appearance of the opercular flap (cf. Fig. 8I and Fig. 8J). In pike, the first expression of *Hand2* can also be seen in the hyoid region (Fig. 8N); however, pike larvae do not develop any prominent hyoid structure similar to bichir and gar. We thus postulated that accelerated hyoid CNC development relates to precocious differentiation of neural crest-derived structures in pike larvae. Consistent with this, Alcian-blue staining revealed that the first detectable cartilaginous element in pike larvae is the hyosymplectic of the hyoid arch origin (Fig. 8O). Taken together, these data demonstrate that acceleration of the hyoid neural crest is associated with early formation of several key species-specific hyoid arch structures in bichir, gar, and pike embryos.

Sterlet cranial neural crest cells constitute a single hyobranchial sheet

Journal Pre-proof

In sterlet, our data revealed the presence of a common hyobranchial sheet of CNC cells (Fig. 4K, O, S; Fig. 7E and Fig. S2). In order to complement our gene expression data with experimental lineage analysis, we took advantage of the accessibility of sterlet embryos and directly tested the exit points and migratory patterns of CNC streams using direct cell labeling with a lipophilic dye. To this end, we microinjected CM-DiI (Fig. 9) into the dorsal midline of the neural folds at selected levels along the anteroposterior axis (Fig. 9A; mandibular: 10/10, hyoid: 13/15). Sterlet embryos were then allowed to develop to stages when CNC cells begin to form migrating streams (Fig. 9A, E, I). We first performed focal microinjection of CM-DiI into the prospective mandibular CNC anterior to rhombomere 3 (cf. Fig. 9B and Fig. 4F); the results confirmed the migratory pattern we previously inferred using neural crest markers (cf. Fig. 9C and Fig. 4; Fig. 7; Fig. S2). At later developmental stages, CM-DiI-positive cells are detected throughout the anterior head and in the presumptive jaws (Fig. 9D-E). Next, we tested whether the hyobranchial sheet emerges from a single exit point. We performed CM-DiI microinjection into the presumptive hyobranchial neural crest population at the dorsal midline of the neural fold (cf. Fig. 9A, F and Fig, 4F, J, R). Consistent with our previous gene expression analyses, the fate-mapping experiment corroborated the presence of a single hyobranchial sheet (Fig. 4K, O, S and Fig. 7E), with CM-DiI-positive cells later contributing to cells of both the hyoid and branchial streams (Fig. 9A, G-I). We next sought to determine the time point at which the hyobranchial sheet separates into the individual hyoid and branchial neural crest streams. Comparison of SOX9 antibody staining (Fig. 10A, D), micro-CT reconstruction of the endodermal epithelium (Fig. 10B, E) and transverse histological sections (Fig. 10C, F) reveals that the separation of the hyobranchial sheet is tightly associated developmentally with morphogenesis of the second (hyo-branchial) pharyngeal pouch (Fig. 10B-C, E-F).

Discussion

In the present study, we analyzed the patterning and migration of cranial neural crest cells in the Senegal Bichir (Cladistia), the sterlet sturgeon (Chondrostei), the tropical gar (Holostei) and the northern pike (Teleostei). These species are representatives of all recent phylogenetic lineages of ray-finned fishes that together exemplify about half of extant vertebrates (Betancur-R et al., 2017; Hughes et al., 2018). While patterns of CNC migration are often assumed to be highly stereotypic across vertebrates (Minoux and Rijli, 2010; Theveneau and Mayor, 2012; Falck et al., 2002), our study reveals significant modifications in the canonical pattern of migration in ray-finned fishes (Fig. 11). This raises the interesting possibility that CNC migratory patterns may be much more variable than commonly assumed from studies of a small number of model organisms, further highlighting the importance of comparative analyses.

Transitional patterns of neurulation

Our examined fish species provide powerful model systems for the study of evolution of neurulation in vertebrates as these embryos utilize modes of neurulation ranging from primary neurulation to neurulation via cavitation (Fig. 1), consistent with an evolutionary transition in this critical developmental process. Our data reveal that bichir embryos undergo primary neurulation when the entire morphogenetic process occurs above the yolk ball, which is apparently similar to the neurulation of salamanders and some frogs (cf. Fig. 1A-D and Schreckenberg and Jacobson, 1975; Eagleson, 1996; Del Pino et al., 2004; Mitgutsch et al., 2009). Therefore, the presence of primary neurulation in bichir may reflect another character shared with lobe-finned fishes. As in bichir, sterlet embryos undergo primary neurulation via rolling up of the neural folds (cf. Fig. 1A-D and Fig. 1E-H). However, the entire morphogenetic process in sterlet takes place within the yolk ball, apparently similar to the neurulation of direct-developing frogs (Olsson et al., 2002). In contrast, gar embryos undergo neurulation via formation of a neural keel, which is characteristic for all teleosts including pike (cf. Fig. 1I-L and Schmitz et al., 1993; Lowery and

Sive, 2004; Pospisilova et al., 2019; Rocha et al., 2019). We next asked when CNC cells begin their migration. Our spatiotemporal analysis of neural crest markers reveals that CNC cells of all examined fish species initiate emigration during early neurulation (cf. Fig. 1 and Fig. 2), similar to that described in frogs (Mitgutsch et al., 2008) and mammals (Tan and Moris-Kay, 1986; Smith, 2001) but contrasting with that of most vertebrates, which typically initiate migration after neural tube closure (Noden, 1988; Horigome et al., 1999; Falck et al., 2002; Diaz et al., 2019). Although neural crest development is tightly connected to morphogenesis of neurulation, our data suggest that the type of neurulation has little or no influence on CNC migratory patterns.

Accelerated hyoid neural crest stream is associated with different hyoid structures in different species

In all vertebrates, cranial neural crest cells migrate in three distinct streams, termed mandibular, hyoid and branchial, that emerge from consecutive positions along the anteroposterior axis (Minoux and Rijli, 2010; Theveneau and Mayor, 2012; Square et al., 2017). While this migratory pattern has been assumed to be stereotypic, our results clearly demonstrate heterochrony in the overall acceleration of the second, hyoid CNC stream. Specifically, in bichir, gar, and pike embryos, cells of the hyoid stream migrate before cells of the first, mandibular stream (Fig. 2A-C, P-R, S-U). In vertebrates, the hyoid stream is usually smaller in size and range compared to the mandibular stream, which occupies the entire rostral head (Couly et al., 1993; Creuzet et al., 2002; Santagati and Rijli, 2003; Piekarski et al., 2014). However, in bichir, our gene expression data suggest that the hyoid CNC constitutes the most prominent neural crest population in the developing head (Fig. 3J-K; Fig. 7A-C) and is the first to reach ventral-most positions in the developing pharyngeal region and the external gills, respectively (Fig. 8A-E). These data further corroborate our previous report (Stundl et al., 2019), showing that accelerated development of the entire hyoid arch segment also involves mesodermal and endodermal tissues, which

together promote advanced morphogenesis of the external gills, forming a crucial structure of bichir embryos and larvae (Kerr, 1907; Kerr, 1919).

Like bichir, gar embryos exhibit prominent heterochrony in the hyoid stream (Fig. 2P-R). While the gar hyoid stream initiates migration first, it does not form the dominant stream. Nevertheless, hyoid CNC cells are the first to reach ventral positions in the developing oropharynx and in the prominent opercular flap, respectively (Fig. 8I). The accelerated hyoid stream thus seems to be developmentally associated with the morphogenesis of large opercular flap (Fig. 8J), which forms a key supplemental respiratory organ in gar larvae (Agassiz, 1878; Balfour and Parker, 1882). We next asked whether, in gar embryos, the development of endoderm and mesoderm is accelerated similar as previously observed in bichir (Stundl et al., 2019). Interestingly, we found that the hyoid pharyngeal endoderm expands laterally, and later contributes to a massive opercular flap of gar embryos (Fig. S3; Minarik et al., 2017). Moreover, the hyoid mesoderm seems to be accelerated as well, as the hyomandibularis muscle is among the first cranial muscles forming in gar (Konstantidinis et al., 2015). Thus, in gar embryos similar to bichir, advanced development of the entire hyoid domain, comprising neural crest, mesoderm, and endoderm, is found to be the case. This apparently is associated with the morphogenesis of a large opercular flap constituting a key secondary breathing structure in gar (Fig. 8J). Interestingly, gar exhibits very similar embryogenesis to the bowfin, and both these representatives of the phylogenetic group Holostei also possess prominent opercular flap with probably the same key influence for their larvae (Dean, 1895; Ballard, 1986; Long and Ballard, 2001; Jaroszewska and Dabrowski, 2009). We thus speculate that bowfin may have a similar accelerated hyoid neural crest stream serving the same function as in gar embryos.

Pike belongs to teleost fishes that represent the vast majority of extant ray-finned fish species. Embryonic development of pike is very similar to other teleosts (Pospisilova et al., 2019), including model organisms like zebrafish or medaka (Kimmel et al., 1995; Iwamatsu,

2004). Despite the high similarity of the early development of pike and other teleosts, our data show that the hyoid CNC stream in pike embryos initiates migration much earlier than the mandibular neural crest stream (Fig. 2S-U) and is the first stream to reach the ventral part of the oropharyngeal region as in bichir and gar (Fig. 8N). We speculate that this advanced development of the hyoid CNC may be associated with a unique early chondrogenesis of the hyosymplectic cartilage in pike (Fig. 8O; Pospisilova et al., 2019) which forms an essential component of jaw attachment in ray-finned fishes (Richter and Underwood, 2018). Only in the whiting (*Merlangius merlangus* Linnaeus, 1758) has a similar process of advanced chondrogenesis been described (de Beer, 1937). Furthermore, gar seems to exhibit the same pattern as well (data not shown). However, this sequence of chondrogenesis might be more common among ray-finned fishes since most studies do not provide enough details on early chondrogenesis (Vandewalle et al., 1999; Borisov et al., 2012). Given that acceleration of the hyoid CNC was observed in representatives of two of three phylogenetic lineages of non-teleost fishes as well as in a representative of teleosts, it is tempting to speculate that such heterochrony in the hyoid CNC represents an ancient common character for all ray-finned fishes.

Journal Pre-proof

Sterlet cranial neural crest cells constitute a single hyobranchial sheet

In contrast to bichir, gar and pike, the hyoid neural crest of sterlet is not accelerated but does display unique morphogenesis in which the hyoid and branchial CNC cells are fused into a single 'hyobranchial sheet' (Fig. 4K, O, S; Fig. 7E and Fig. S2). This subpopulation becomes separated into individual streams only later in concert with second pharyngeal pouch morphogenesis (Fig. 10A-F), similar to the segregation of other migratory neural crest streams (Grevellec and Tucker, 2010). Whereas in most vertebrates, the otic capsule physically separates the hyoid and branchial neural crest streams, the formation of the otic capsule seems

delayed in sterlet embryos (Fig. 10C, F). Therefore, the hyoid and branchial CNC of sterlet are initially unsegmented and migrate into the presumptive pharyngeal region in a sheet-like fashion, analogous to the common branchial stream of lamprey embryos (McCauley and Bronner-Fraser, 2003; Square et al., 2017). Possible evolutionary implications of this variation in the migratory pattern in sterlet are unclear, but it further supports the importance of pharyngeal endoderm morphogenesis for the segregation of CNC streams (Piotrowski and Nüsslein-Volhard, 2000; McCauley and Bronner-Fraser, 2003; Cerny et al., 2004).

Unique pattern of cranial neural crest migration among vertebrates

While dogma has it that CNC migration patterns are highly conserved across vertebrates, our data show a clear departure from this concept. While there are clearly three topographically conserved streams among all vertebrates (Fig. 11; Falck et al., 2002; Cerny et al., 2004; Square et al., 2017), we show that there is heterochrony of the hyoid CNC stream associated with early morphogenesis of key hyoid structures like external gills (bichir), large opercular flap (gar), or first forming cartilage (pike) essential for the hyostylic jaw suspension. However, this hyoid heterochrony has not yet been observed in fish model organisms such as zebrafish or medaka (Schilling and Kimmel, 1994; Stewart et al., 2006; Nagao et al., 2018; Rocha et al., 2019). This raises the question of what represents the ancestral state: do the observed heterochronic alterations in CNC migratory patterns represent an ancestral state of ray-finned fish development? or even an ancestral state of gnathostome development? One possibility is that this heterochrony exists in model fish but has been missed due to their rapid development. For example, twist1a expression is present in the premigratory CNC cells at the 2-somite stage of zebrafish, and the locations of twist1a-positive cells may well correspond to the hyoid region (Yeo et al., 2009) or may represent a posterior part of the mandibular CNC stream. Given the accelerated hyoid CNC stream found in all fish species in the present study (except the sterlet)

and presumably in other teleost fishes, it seems likely that the heterochrony of hyoid CNC might represent an ancient plesiomorphic character of all ray-finned fishes (Fig. 11). Thus, the question is whether we can find similar heterochrony of the hyoid CNC associated with the development of specific hyoid structures in the other gnathostomes. Interestingly, the hyostylic jaw suspension is also characteristic for cartilaginous fishes. Based on published data, it appears that they do not possess heterochrony in hyoid CNC (Kuratani and Horigome, 2000; Compagnucci et al., 2013; Johanson et al., 2015; Gillis et al., 2017; Martik et al., 2019). However, this may be due to little-studied embryonic development of different groups of cartilaginous fishes and a lack of focus on the details of CNC migration. Nevertheless, it is possible to reveal the developmental potential of the hyoid domain for the morphogenesis of the respiratory structure in the chimera, where gill filaments and especially opercular flap form on the outside of the hyoid arch (Didier et al., 1998; Barske et al., 2020) and thus could perform the same function as the gar opercular flap. This hyoid opercular flap remains in early embryogenesis of amniotes (Richardson et al., 2012), suggesting that it was present in the common ancestor. It remains to be determined whether these hyoid structures are also developmentally associated with the modifications of the hyoid CNC. In contrast, in sterlet, we identified the hyoid and branchial CNC are initially unsegmented and constitute a single hyobranchial sheet which migrates in a sheet-like fashion. This appears to be analogous to the migration of a common branchial CNC stream of lamprey emerging from a broad domain from 5th to 7th rhombomeres and part of the spinal cord (Kuratani et al., 1998; Square et al., 2017). These CNC sheets become segregated in concert with pharyngeal pouch morphogenesis in both sterlet and lamprey. The question arises as to whether a sister species of sturgeon, the paddlefish, has a similar pattern of CNC migration, which could indicate whether it is a common feature of Chondrosteans (Acipenseriformes) or not (Inoue et al., 2003; Near et al., 2012), but cannot be answered without a more in-depth analysis of CNC migration (Bemis and Grande, 1992). Interestingly, a similar constitution unsegmented hyoid and branchial CNC streams can

be found in several species of frogs at early neurula stages (Olsson and Hanken, 1996; Del Pino and Medina, 1998; Mitgutsch et al., 2008; 2009) but the subsequent division of this CNC subpopulation does not appear to be influenced by the morphogenesis of hyo-branchial pharyngeal pouch as in sterlet. In the future work, it would be interesting to analyze receptor-ligand pairs (e.g., eph/ephrins or neuropillins/semaphorins) which may be important for the separating neural crest streams, and the establishment of intervening "neural crest free" zones.

Conclusions

In conclusion, we have performed a comparative analysis of cranial neural crest migration and patterning in representatives of all phylogenetic lineages of ray-finned fishes (bichir - Cladistia, sterlet - Chondrostei, gar - Holostei, and pike - Teleosts) (Fig. 11). Embryos of ray-finned fishes reveal several important variations in the migratory pattern of CNC cells that previously were assumed to be highly stereotypic and conserved in vertebrates. Accelerated development of the hyoid stream of neural crest cells was identified in bichir, gar and pike embryos, always associated with prominent morphogenesis of important species-specific structures of the hyoid arch origin. A single hyobranchial sheet of CNC cells was identified in sterlet embryos, where separate hyoid and branchial streams form only later following prospective morphogenesis of the hyo-branchial pharyngeal pouch. Together, our results reveal unexpected variability in the timing and sequence of CNC emergence and subsequent migratory patterns in several ray-finned species. Our findings thus suggest that vertebrate craniofacial diversity may be associated with heterochronic and heterotopic alterations in migratory patterns of CNC cells as a prime mode of producing varied craniofacial phenotypes.

Acknowledgements

We thank Vojtěch Miller and Karel Kodejš for the bichir colony care and logistic support; Roman Franěk, Michaela Fučíková, David Gela, Martin Kahanec and Marek Rodina for the sterlet spawns; Lenin Arias-Rodriguez and Adriana Osorio-Pérez for the gar spawns; Radek Holcman for the northern pike spawns; Peter Fabian, Martin Minařík and Brian D. Metscher for technical assistance; David Jandzik for the generous gift of primer sequences of Hand2_Ps; Vladimir Soukup and Jana Štundlová for critical reading of the manuscript. Special thanks are due to Radek Šanda for the support and continuous interest in our work. This study was supported by the European Union's Horizon 2020 research and innovation program under the Marie Skłodowska-Curie grant agreement No. 897949 (to JS), the Charles University grant GAUK 1448514 (to JS), NIH R35NS111564 (to MEB), the Czech Science Foundation GACR 19-18634S (to RC), and the Ministry of Education, Youth and Sports of the Czech Republic—project CENAKVA LM2018099 and Biodiversity CZ.02.1.01/0.0/0.0/16_025/0007370) (to MP).

Journal Pre-proof

References

Agassiz, A., 1878. The Development of Lepidosteus . Part I. Proc. Am. Acad. Arts Sci. 14, 65–76. https://doi.org/10.2307/25138527

Baker, C.V.H., Bronner-Fraser, M., 1997. The origins of the neural crest. Part I: embryonic induction. Mech. Dev. 69, 3–11. https://doi.org/10.1016/S0925-4773(97)00132-9

Balfour, F. M., Parker, W.N., 1882. VII. On the structure and development of Lepidosteus. Philos. Trans. R. Soc. B Biol. Sci. 173, 359–442. https://doi.org/10.1098/rstl.1882.0008

Ballard, W.W., 1986. Stages and rates of normal development in the holostean Fish, Amia calva. J. Exp. Zool. 238, 337–354. https://doi.org/10.1002/jez.1402380308

Ballard, W.W., Mellinger, J., Lechenault, H., 1993. A Series of Normal Stages for Development of Scyliorhinus canicula , the Lesser Spotted Dogfish (Chondrichthyes: Scyliorhinidae). J. Exp. Zool. 267, 318–336. https://doi.org/10.1002/jez.1402670309

Barske, L., Fabian, P., Hirschberger, C., Jandzik, D., Square, T., Xu, P., Nelson, N., Yu, H. V., Medeiros, D.M., Gillis, J.A., Crump, J.G., 2020. Evolution of vertebrate gill covers via shifts in an ancient Pou3f3 enhancer Lindsey Barske. bioRxiv 1–36. https://doi.org/https://doi.org/10.1101/2020.01.27.918193

Basch, M.L., Bronner-Fraser, M., García-Castro, M.I., 2006. Specification of the neural crest occurs during gastrulation and requires Pax7. Nature 441, 1–5. https://doi.org/10.1038/nature04684

Bemis, W.E., Grande, L., 1992. Early Development of the Actinopterygian Head. I. External Development and Staging of the Paddlefish Polyodon spathula. J. Morphol. 213, 47–83. https://doi.org/10.1002/jmor.1052130106

Betancur-R, R., Wiley, E.O., Arratia, G., Acero, A., Bailly, N., Miya, M., Lecointre, G., Ortí, G., 2017. Phylogenetic classification of bony fishes. BMC Evol. Biol. 17, 1–40. https://doi.org/10.1186/s12862-017-0958-3

Betters, E., Charney, R.M., Garcia-Castro, M.I., 2018. Early speci fi cation and development of rabbit neural crest cells. Dev. Biol. 444, Suppl 1, S181–S192. https://doi.org/10.1016/j.ydbio.2018.06.012

Borisov, V.B., Shkil, F.N., Abdissa, B., Smirnov, S. V., 2012. Development of the Cranium in the Large African Hexaploid Barb Labeobarbus (=Barbus) intermedius (Cyprinidae; Teleostei). J. Ichthyol. 52, 838–860. https://doi.org/10.1134/S0032945212110021

Bronner, M.E., Ledouarin, N.M., 2012. Development and evolution of the neural crest: An overview. Dev. Biol. 366, 2–9. https://doi.org/10.1016/j.ydbio.2011.12.042

Carmona-Fontaine, C., Matthews, H.K., Kuriyama, S., Moreno, M., Dunn, G., Parsons, M., Stern, C.D., Mayor, R., 2008. Contact inhibition of locomotion in vivo controls neural crest directional migration. Nature 456, 957–961. https://doi.org/10.1038/nature07441

Cerny, R., Cattell, M., Sauka-Spengler, T., Bronner-Fraser, M., Yu, F., Meulemans Medeiros, D., 2010. Evidence for the prepattern/cooption model of vertebrate jaw evolution. Proc. Natl. Acad. Sci. 107, 17262–17267. https://doi.org/10.1073/pnas.1009304107

Cerny, R., Lwigale, P., Ericsson, R., Meulemans, D., Epperlein, H.-H., Bronner-Fraser, M., 2004. Developmental origins and evolution of jaws: new interpretation of “maxillary” and “mandibular.” Dev. Biol. 276, 225–236. https://doi.org/10.1016/j.ydbio.2004.08.046

Cerny, R., Meulemans, D., Berger, J., Wilsch-Bräuninger, M., Kurth, T., Bronner-Fraser, M., Epperlein, H.-H., 2004. Combined intrinsic and extrinsic influences pattern cranial neural crest migration and pharyngeal arch morphogenesis in axolotl. Dev. Biol. 266, 252–269. https://doi.org/10.1016/j.ydbio.2003.09.039

Cheung, M., Briscoe, J., 2003. Neural crest development is regulated by the transcription factor. Development 130, 5681–5693. https://doi.org/10.1242/dev.00808

Compagnucci, C., Debiais-Thibaud, M., Coolen, M., Fish, J., Griffin, J.N., Bertocchini, F., Minoux, M., Rijli, F.M., Borday-Birraux, V., Casane, D., Mazan, S., Depew, M.J., 2013. Pattern and polarity in the development and evolution of the gnathostome jaw: Both conservation and heterotopy in the branchial arches of the shark, Scyliorhinus canicula. Dev. Biol. 377, 428–448. https://doi.org/10.1016/j.ydbio.2013.02.022

Cooper, M.S., Virta, V.C., 2007. Evolution of Gastrulation in the Ray-Finned (Actinopterygian) Fishes 308B: 591–608. https://doi.org/10.1002/jez.b.21142

Couly, G.F., Coltey, P.M., Le Douarin, N.M., 1993. The triple origin of skull in higher vertebrates: a study in quail-chick chimeras. Development 117, 409–429.

Creuzet, S., Couly, G., Vincent, C., Le Douarin, N.M., 2002. Negative effect of Hox gene expression on the development of the neural crest-derived facial skeleton. Development 129, 4301–4313.

Crump, J.G., Maves, L., Lawson, N.D., Weinstein, B.M., Kimmel, C.B., 2004. An essential role for Fgfs in endodermal pouch formation influences later craniofacial skeletal patterning. Development 131, 5703–5716. https://doi.org/10.1242/dev.01444

David, N.B., Saint-Etienne, L., Tsang, M., Schilling, T.F., Rosa, F.M., 2002. Requirement for endoderm and FGF3 in ventral head skeleton formation. Development 129, 4457–4468.

de Beer, G.R., 1937. The development of the vertebrate skull. Oxford University Press, London.

Dean, B., 1895. The early development of Gar-pike and Sturgeon. J. Morphol. XI. https://doi.org/10.1002/jmor.1050110102

Del Pino, E., Medina, A., 1998. Neural development in the marsupial frog Gastrotheca riobambae. Int. J. Dev. Biol. 42, 723–731.

Del Pino, E., Ávila, M.-E., Pérez, O.D., Benítez, M.-S., Alarcón, I., Noboa, V., Moya, I.M., 2004. Development of the dendrobatid frog Colostethus machalilla. Int. J. Dev. Biol. 48, 663–670. https://doi.org/10.1387/ijdb.041861ed

Dettlaff, T.A., Ginsburg, A.S., Schmalhausen, O.I., 1993. Sturgeon Fishes-Developmental Biology and Aquaculture. Springer

Diaz Jr, R. E.; Shylo, N. A.; Roellig, D.; Bronner, M., Trainor, P.A., 2019. Filling in the phylogenetic gaps: Induction, migration, and differentiation of neural crest cells in a squamate reptile, the Veiled Chameleon (Chamaeleo calyptratus). Dev. Dyn. 248, 709–727. https://doi.org/10.1002/dvdy.38.

Didier, D.A., LeClair, E.E., Vanbuskirk, D.R., 1998. Embryonic Staging and External Features of Development of the Chimaeroid Fish , Callorhinchus milii (Holocephali, Callorhinchidae). J. Morphol. 236, 25–47. https://doi.org/10.1002/(SICI)1097-4687(199804)236:1<25::AID-JMOR2>3.0.CO;2-N

Diedhiou, S., Bartsch, P., 2009. Staging of the early development of Polypterus (Cladistia: Actinopterygii), in: Development of Non-Teleost Fishes. pp. 104–169.

Donoghue, P.C.J., Keating, J.N., 2014. Early Vertebrate Evolution. Palaeontology 57, 1–15. https://doi.org/10.1111/pala.12125

Eagleson, G.W., 1996. Developmental neurobiology of the anterior areas in amphibians: urodele perspectives. Int. J. Dev. Biol. 40, 735–743.

Falck, P., Hanken, J., Olsson, L., 2002. Cranial neural crest emergence and migration in the Mexican axolotl (Ambystoma mexicanum). Zoology 105, 195–202. https://doi.org/10.1078/0944-2006-00079

Forey, P., Janvier, P., 1994. Evolution of the early vertebrates. Sci. Am. 82, 554–565.

Gans, C., Northcutt, R.G., 1983. Neural Crest and the Origin of Vertebrates: A New Head. Science 220, 268–274. doi: 10.1126/science.220.4594.268

Gillis, J.A., Alsema, E.C., Criswell, K.E., 2017. Trunk neural crest origin of dermal denticles in a cartilaginous fish. Proc. Natl. Acad. Sci. 18, 1–6. https://doi.org/10.1073/pnas.1713827114

Gouignard, N., Andrieu, C., Theveneau, E., 2018. Neural crest delamination and migration: Looking forward to the next 150 years. Genesis 56:e23107. https://doi.org/10.1002/dvg.23107

Graham, A., 2008. Deconstructing the pharyngeal metamere. J. Exp. Zool. Part B Mol. Dev. Evol. 310B, 336–344. https://doi.org/10.1002/jez.b.21182

Green, S.A., Simoes-Costa, M., Bronner, M.E., 2015. Evolution of vertebrates as viewed from the crest. Nature 520, 474–482. https://doi.org/10.1038/nature14436

Grevellec, A., Tucker, A.S., 2010. Seminars in Cell & Developmental Biology The pharyngeal pouches and clefts: Development, evolution, structure and derivatives. Semin. Cell Dev. Biol. 21, 325–332. https://doi.org/10.1016/j.semcdb.2010.01.022

Hall, B.K., 2009. Neural Crest Derivatives, in: The Neural Crest and Neural Crest Cells in Vertebrate Development and Evolution. pp. 159–268.

Harrington, M.J., Hong, E., Brewster, R., 2009. Comparative Analysis of Neurulation: First Impressions Do Not Count. Mol. Reprod. Dev. 76, 954–965. https://doi.org/10.1002/mrd.21085

Hockman, D., Chong-Morrison, V., Green, S.A., Gavriouchkina, D., Candido-Ferreira, I., Ling, I.T.C., Williams, R.M., Amemiya, C.T., Smith, J.J., Bronner, M.E., Sauka-Spengler, T., 2019. A genome-wide assessment of the ancestral neural crest gene regulatory network. Nat. Commun. 10, 1–15. https://doi.org/10.1038/s41467-019-12687-4

Horigome, N., Myojin, M., Ueki, T., Hirano, S., Aizawa, S., Kuratani, S., 1999. Development of Cephalic Neural Crest Cells in Embryos of Lampetra japonica, with Special Reference to the Evolution of the Jaw. Dev. Biol. 207, 287–308. https://doi.org/10.1006/dbio.1998.9175

Hughes, L.C., Ortí, G., Huang, Y., Sun, Y., Baldwin, C.C., Thompson, A.W., Arcila, D., Betancur-R., R., Li, C., Becker, L., Bellora, N., Zhao, X., Li, X., Wang, M., Fang, C., Xie, B., Zhou, Z., Huang, H., Chen, S., Venkatesh, B., Shi, Q., 2018. Comprehensive phylogeny of ray-finned fishes (Actinopterygii) based on transcriptomic and genomic data. Proc. Natl. Acad. Sci. 115, 6249–6254. https://doi.org/10.1073/pnas.1719358115

Inoue, J.G., Miya, M., Tsukamoto, K., Nishida, M., 2003. Basal actinopterygian relationships : a mitogenomic perspective on the phylogeny of the " ancient fish". Mol. Phylogenet. Evol. 26, 110–120. https://doi.org/10.1016/S1055-7903(02)00331-7

Iwamatsu, T., 2004. Stages of normal development in the medaka Oryzias latipes. Mech. Dev. 121, 605–618. https://doi.org/10.1016/j.mod.2004.03.012

Jaroszewska, M., Dabrowski, K., 2009. Early Ontogeny of Semionotiformes and Amiiformes (Neopterygii: Actinopterygii), in: Development of Non-Teleost Fishes. pp. 230–274.

Johanson, Z., Boisvert, C., Maksimenko, A., Currie, P. Trinajstic, K., 2015. Development of the Synarcual in the Elephant Sharks (Holocephali; Chondrichthyes): Implications for Vertebral Formation and Fusion. PLoS One 10(9):e0135138., 1–19. https://doi.org/10.1371/journal.pone.0135138

Kerr, J.G., 1907. The development of Polypterus senegalus Cuvier, in: The Work of John Samuel Budgett. Cambridge University Press.

Kerr, J.G., 1919. Textbook of Embryology. Vol II. Vertebrata with the exception of mammalia. Macmillan and CO., London.

Kimmel, C.B., Ballard, W.W., Kimmel, S.R., Ullmann, B., Schilling, T.F., 1995. Stages of embryonic development of the zebrafish. Dev. Dyn. 203, 253–310. https://doi.org/10.1002/aja.1002030302

Konstantinidis, P., Warth, P., Naumann, B., Metscher, B., Hilton, E.J., Olsson, L., 2015. The Developmental Pattern of the Musculature Associated with the Mandibular and Hyoid Arches in the Longnose Gar, Lepisosteus osseus (Actinopterygii, Ginglymodi, Lepisosteiformes). Copeia 103, 920–932. https://doi.org/10.1643/OT-14-195

Kulesa, P.M., Bailey, C.M., Kasemeier-Kulesa, J.C., McLennan, R., 2010. Cranial neural crest migration: New rules for an old road. Dev. Biol. 344, 543–554. https://doi.org/10.1016/j.ydbio.2010.04.010

Kunz, Y.W., Luer, C.A., Kapoor, B.G., 2009. Development of Non-Teleost Fishes. Science Publishers, Enfield.

Kuo, B.R., Erickson, C.A., 2010. Regional differences in neural crest morphogenesis Regional differences in neural crest morphogenesis. Cell Adh. Migr. 4, 567–585. https://doi.org/10.4161/cam.4.4.12890

Kuratani, S., Horigome, N., Ueki, T., Aizawa, S., 1998. Stereotyped Axonal Bundle Formation and Neuromeric Patterns in Embryos of a Cyclostome , Lampetra japonica. J. Comp. Neurol. 391, 99–114.

Kuratani, A., Kuratani, S., Horigome, N., 2000. Developmental Morphology of Branchiomeric Nerves in a Cat Shark, Scyliorhinus torazame, with Special Reference to Rhombomeres, Cephalic Mesoderm, and Distribution Patterns of Cephalic Crest Cells. Zoolog. Sci. 17, 893–909. https://doi.org/10.2108/zsj.17.893

Le Douarin, N. M., Dupin, E., 2014. The Neural Crest, a Fourth Germ Layer of the Vertebrate Embryo: Significance in Chordate Evolution, in: Trainor, P.A. (Ed.), Neural Crest Cells. Elsevier, pp. 3–26.

Long, W.L., Ballard, W.W., 2001. Normal embryonic stages of the Longnose Gar, Lepisosteus osseus. BMC Dev. Biol. 1. https://doi.org/10.1186/1471-213X-1-6

Lowery, L.A., Sive, H., 2004. Strategies of vertebrate neurulation and a re-evaluation of teleost neural tube formation. Mech. Dev. 121, 1189–1197. https://doi.org/10.1016/j.mod.2004.04.022

Martik, M.L., Bronner, M.E., 2017. Regulatory Logic Underlying Diversification of the Neural Crest. Trends Genet. 33, 715–727. https://doi.org/10.1016/j.tig.2017.07.015

Martik, M.L., Gandhi, S., Uy, B.R., Gillis, J.A., Green, S.A., Simoes-Costa, M., Bronner, M.E., 2019. Evolution of the new head by gradual acquisition of neural crest regulatory circuits. Nature 574, 675–678. https://doi.org/10.1038/s41586-019-1691-4

McCauley, D.W., Bronner-Fraser, M., 2003. Neural crest contributions to the lamprey head. Development 130, 2317–2327. https://doi.org/10.1242/dev.00451

Metscher, B.D., 2009. MicroCT for developmental biology: A versatile tool for high-contrast 3D imaging at histological resolutions. Dev. Dyn. 238, 632–640. https://doi.org/10.1002/dvdy.21857

Meulemans Medeiros, D., 2013. The evolution of the neural crest: new perspectives from lamprey and invertebrate neural crest-like cells. WIREs Dev. Biol. 2, 1–15. https://doi.org/10.1002/wdev.85

Minarik, M., Stundl, J., Fabian, P., Jandzik, D., Metscher, B.D., Psenicka, M., Gela, D., Osorio-Pérez, A., Arias-Rodriguez, L., Horácek, I., Cerny, R., 2017. Pre-oral gut contributes to facial structures in non-teleost fishes. Nature 547, 209–212. https://doi.org/10.1038/nature23008

Minoux, M., Rijli, F.M., 2010. Molecular mechanisms of cranial neural crest cell migration and patterning in craniofacial development. Development 137, 2605–2621. https://doi.org/10.1242/dev.040048

Mitgutsch, C., Olsson, L., Haas, A., 2009. Early embryogenesis in discoglossoid frogs: a study of heterochrony at different taxonomic levels. J. Zool. Syst. Evol. Res. 47, 248–257. https://doi.org/10.1111/j.1439-0469.2008.00502.x

Mitgutsch, C., Piekarski, N., Olsson, L., Haas, A., 2008. Heterochronic shifts during early cranial neural crest cell migration in two ranid frogs. Acta Zool. 89, 69–78. https://doi.org/10.1111/j.1463-6395.2007.00295.x

Mori-Akiyama, Y., Akiyama, H., Rowitch, D.H., de Crombrugghe, B., 2003. Sox9 is required for determination of the chondrogenic cell lineage in the cranial neural crest. Proc. Natl. Acad. Sci. 100, 9360–9365. https://doi.org/10.1073/pnas.1631288100

Nagao, Y., Takada, H., Miyadai, M., Adachi, T., Seki, R., Kamei, Y., Hara, I., Taniguchi, Y., Naruse, K., Hibi, M., Kelsh, R.N., Hashimoto, H., 2018. Distinct interactions of Sox5 and Sox10 in fate specification of pigment cells in medaka and zebrafish. Plos Genet. 14:e100726. https://doi.org/DOI: 10.1371/journal.pgen.1007260

Near, T.J., Eytan, R.I., Dornburg, A., Kuhn, K.L., Moore, J.A., Davis, M.P., Wainwright, P.C., Friedman, M., Smith, W.L., 2012. Resolution of ray-finned fish phylogeny and timing of diversification. Proc. Natl. Acad. Sci. 109, 13698–13703. https://doi.org/10.1073/pnas.1206625109

Nieto, M.A., Sechrist, J., Wilkinson, D.G., Bronner-Fraser, M., 1995. Relationship between spatially restricted Krox-20 gene expression in branchial neural crest and segmentation in the chick embryo hindbrain. EMBO J. 14, 1697–1710. https://doi.org/10.1002/j.1460-2075.1995.tb07159.x

Noden, D.M., 1988. Interactions and fates of avian craniofacial mesenchyme. Development 103, 121–140.

Northcutt, G., Gans, C., 1983. The Genesis of Neural Crest and Epidermal Placodes: A Reinterpretation of Vertebrate Origins. Q. Rev. Biol. 58, 1–28.

Northcutt, R.G., 2005. The New Head Hypothesis Revisited. J. Exp. Zool. (Mol Dev Evol) 304B, 274–297. https://doi.org/10.1002/jez.b.21063

Odelin, G., Faure, E., Coulpier, F., Di Bonito, M., Bajolle, F., Studer, M., Avierinos, J.-F., Charnay, P., Topilko, P., Zaffran, S., 2018. Krox20 defines a subpopulation of cardiac neural crest cells contributing to arterial valves and bicuspid aortic valve. Development 145, 1–10. https://doi.org/10.1242/dev.151944

Olsson, L., Hanken, J., 1996. Cranial Neural-Crest Migration and Chondrogenic Fate in the Oriental Fire-Bellied Toad Bombina orientalis : Defining the Ancestral Pattern of Head Development in Anuran Amphibians. J. Morphol. 229, 105–120. https://doi.org/10.1002/(SICI)1097-4687(199607)229:1<105::AID-JMOR7>3.0.CO;2-2

Olsson, L., Moury, J.D., Carl, T.F., Håstad, O., Hanken, J., 2002. Cranial neural crest-cell migration in the direct-developing frog, Eleutherodactylus coqui: molecular heterogeneity within and among migratory streams. Zoology 105, 3–13. https://doi.org/10.1078/0944-2006-00051

Patthey, C., Gunhaga, L., Edlund, T., 2008. Early Development of the Central and Peripheral Nervous Systems Is Coordinated by Wnt and BMP Signals. PLoS One 3, 2–11. https://doi.org/10.1371/journal.pone.0001625

Piekarski, N., Gross, J.B., Hanken, J., 2014. Evolutionary innovation and conservation in the embryonic derivation of the vertebrate skull. Nat. Commun. 5, 1–9. https://doi.org/10.1038/ncomms6661

Piotrowski, T., Nüsslein-Volhard, C., 2000. The endoderm plays an important role in patterning the segmented pharyngeal region in zebrafish (Danio rerio). Dev. Biol. 225, 339–356. https://doi.org/10.1006/dbio.2000.9842

Pospisilova, A., Miller, V., Holcman, R., Šanda, R., Stundl, J., 2019. Embryonic and larval development of the northern pike: An emerging fish model system for evo-devo research. J. Morphol. 280, 1118–1140. https://doi.org/10.1002/jmor.21005

Richardson, J., Shono, T., Okabe, M., Graham, A., 2012. The presence of an embryonic opercular flap in amniotes. Proc. R. Soc. B Biol. Sci. 279, 224–229. https://doi.org/10.1098/rspb.2011.0740

Richter, M., Underwood, C., 2018. Origin, Development and Evolution of the Fish Skull, in: Johanson, Z., Underwood, C., Richter, M. (Eds.), Evolution and Development of Fishes. pp. 144–159.

Rocha, M., Singh, N., Ahsan, K., Beiriger, A., Prince, V.E., 2019. Neural crest development: insights from the zebrafish. Dev. Dyn. 249, 1–24. https://doi.org/10.1002/dvdy.122

Rondeau, E.B., Minkley, D.R., Leong, J.S., Messmer, A.M., Jantzen, J.R., von Schalburg, K.R., Lemon, C., Bird, N.H., Koop, B.F., 2014. The genome and linkage map of the northern pike (Esox lucius):

Conserved synteny revealed between the salmonid sister group and the neoteleostei. PLoS One 9. https://doi.org/10.1371/journal.pone.0102089

Rothstein, M., Bhattacharya, D., Simoes-Costa, M., 2018. The molecular basis of neural crest axial identity. Dev. Biol. 444, S170–S180. https://doi.org/10.1016/j.ydbio.2018.07.026

Santagati, F., Rijli, F.M., 2003. Cranial Neural Crest and the Building of the Vertebrate Head. Nat. Rev. Neurosci. 4, 806–820. https://doi.org/10.1038/nrn1221

Sauka-Spengler, T., Bronner-Fraser, M., 2008. A gene regulatory network orchestrates neural crest formation. Nat. Rev. Mol. Cell Biol. 9, 557–568. https://doi.org/10.1038/nrm2428

Schilling, T.F., Kimmel, C.B., 1994. Segment and cell type lineage restrictions during pharyngeal arch development in the zebrafish embryo. Development 120, 483–494.

Schmitz, B., Papan, C., Campos-Ortega, J.A., 1993. Neurulation in the anterior trunk region of the zebrafish Brachydanio rerio. Roux's Arch. Dev. Biol. 202, 250–259.

Schneider, R.A., 2018. Neural crest and the origin of species-specific pattern. Genesis 56:e23219, 1–33. https://doi.org/10.1002/dvg.23219

Schreckenberg, G.M., Jacobson, A.G., 1975. Normal Stages of Development Ambystoma of the Axolotl, mexicanum. Dev. Biol. 42, 391–400. https://doi.org/10.1016/0012-1606(75)90343-7

Simoes-Costa, M., Bronner, M.E., 2013. Insights into neural crest development and evolution from genomic analysis. Genome Res. 23, 1069–1080. https://doi.org/10.1101/gr.157586.113

Simões-Costa, M., Bronner, M.E., 2015. Establishing neural crest identity: a gene regulatory recipe. Development 142, 242–257. https://doi.org/10.1242/dev.105445

Simões-Costa, M., Tan-Cabugao, J., Antoshechkin, I., Sauka-Spengler, T., Bronner, M.E., 2014. Transcriptome analysis reveals novel players in the cranial neural crest gene regulatory network. Genome Res. 24, 281–290. https://doi.org/10.1101/gr.161182.113.

Smith, K.K., 2001. Early development of the neural plate, neural crest and facial region of marsupials. J. Anat. 199, 121–131. https://doi.org/10.1046/j.1469-7580.2001.19910121.x

Soukup, V., Horácek, I., Cerny, R., 2013. Development and evolution of the vertebrate primary mouth. J. Anat. 222, 79–99. https://doi.org/10.1111/j.1469-7580.2012.01540.x

Square, T., Jandzik, D., Cattell, M., Coe, A., Doherty, J., Meulemans Medeiros, D., 2015. Evolution of Developmental Control Mechanisms A gene expression map of the larval Xenopus laevis head reveals developmental changes underlying the evolution of new skeletal elements. Dev. Biol. 397, 293–304. https://doi.org/10.1016/j.ydbio.2014.10.016

Square, T., Jandzik, D., Romášek, M., Cerny, R., Meulemans Medeiros, D., 2017. The origin and diversi fi cation of the developmental mechanisms that pattern the vertebrate head skeleton. Dev. Biol. 427, 219–229. https://doi.org/10.1016/j.ydbio.2016.11.014

Stewart, R.A., Arduini, B.L., Berghmans, S., George, R.E., Kanki, J.P., Henion, P.D., Look, A.T., 2006. Zebrafish foxd3 is selectively required for neural crest specification , migration and survival. Dev. Biol. 292, 174–188. https://doi.org/10.1016/j.ydbio.2005.12.035

Stundl, J., Pospisilova, A., Jandzik, D., Fabian, P., Dobiasova, B., Minarik, M., Metscher, B.D., Soukup, V., Cerny, R., 2019. Bichir external gills arise via heterochronic shift that accelerates hyoid arch development. Elife 8:e43531, 1–13. https://doi.org/10.7554/eLife.43531

Szabó, A., Mayor, R., 2018. Mechanisms of Neural Crest Migration. Annu. Rev. Genet. 52, 43–63. https://doi.org/10.1146/annurev-genet-120417-031559

Takeuchi, M., Takahashi, M., Okabe, M., Aizawa, S., 2009. Germ layer patterning in bichir and lamprey; an insight into its evolution in vertebrates. Dev. Biol. 332, 90–102. https://doi.org/10.1016/j.ydbio.2009.05.543

Tan, S.S., Morriss-Kay, G.M., 1986. Analysis of cranial neural crest cell migration and early fates in postimplantation rat chimaeras. Development. Morphol. 98, 21–58.

Taylor, W.R., Van Dyke, G.C., 1985. Revised procedures for staining and clearing small fishes and other vertebrates for bone and cartilage study. Cybium 107–119.

Theveneau, E., Mayor, R., 2012. Neural crest delamination and migration: From epithelium-to-mesenchyme transition to collective cell migration. Dev. Biol. 366, 34–54. https://doi.org/10.1016/j.ydbio.2011.12.041

Vandewalle, P., Chikou, A., Laleyé, P., Parmentier, E., Huriaux, F., Focant, B., 1999. Early development of the chondrocranium in Chrysichthys auratus. J. Fish Biol. 55, 795–808. https://doi.org/10.1111/j.1095-8649.1999.tb00718.x

Wilkinson, D.G., Bhatt, S., Cook, M., Boncinelli, E., Krumlauf, R., 1989. Segmental expression of Hox-2 homoeobox-containing genes in the developing mouse hindbrain. Nature 341, 405–409. https://doi.org/10.1038/341405a0

Yeo, G.H., Cheah, F.S.H., Winkler, C., Jabs, E.W., Venkatesh, B., Chong, S.S., 2009. Phylogenetic and evolutionary relationships and developmental expression patterns of the zebrafish twist gene family. Dev. Genes Evol. 219, 289–300. https://doi.org/10.1007/s00427-009-0290-z

Figures legends

Fig. 1. *Transitional patterns in neurulation of non-teleost fishes.* (A-L) Whole mount dorsal view at neurulation in bichir (A-D), sterlet (E-H) and gar (I-L). es, embryonic shield; ez, evacuation zone; mes, mesencephalon; nf, neural fold; nk, neural keel; np, neural plate; pog, pre-oral gut; pron, pronephros; pros, prosencephalon; rhom, rhombencephalon; sgc, subgerminal cavity; ypl, yolk plug.

Fig. 2. *Accelerated emigration of CNC cells and heterochronic development of hyoid CNC cells*. *Sox9* expression demonstrates that in bichir (A-C), gar (P-R), and pike (S-U), the hyoid CNC cells are uniquely accelerated in their migration compared to the mandibular CNC cells. (A, D, G, J, M, P, S, V) Cranial expression of *Sox9* in CNC cells in bichir (A, D), sterlet (G, J), gar (M, P), and pike (S, V). White dotted lines indicate the section planes through the mandibular (B, E, H, K, N, Q, T, W) and hyoid domains (C, F, I, L, O, R, U, X), respectively. Identical sections stained with DAPI are marked by ('). White arrowheads

mark the leading edge of the CNC streams. nf, neural fold; ng, neural groove; nk, neural keel; np, neural plate; not, notochord; nt, neural tube.

Fig. 3. *Expression summary of neural crest markers in CNC cells of the Senegal Bichir from the specification through the late phase of migration.* (A-D) SEM and micro-CT images showing dorsal (A-C) and lateral (D) views of CNC developmental stages. (E-H) *Krox20* expression showing position of rhombomere 3 and 5. Dorsal (I-K, M-O, Q-S) and lateral (L, P, T) views of embryos after in situ hybridization for cranial neural crest-specific transcription factors across developmental time-course. White arrowheads mark the pre-oral gut. Asterisks mark exit points of mandibular substreams. B, branchial NC stream; exg, external gill; H, hyoid NC stream; Ma, mandibular NC stream; optv, optic vesicle; otv, otic vesicle; pp1, spiraculum; r3, rhombomere 3; r5, rhombomere 5.

Fig. 4. *Expression summary of neural crest markers in CNC cells of the sterlet sturgeon from the specification through the late phase of migration.* (A-D) SEM and micro-CT images showing dorsal views (A-D) of CNC developmental stages. (E-H) *Krox20* expression showing position of rhombomere 3 and 5. (I-X) Dorsal views of embryos after in situ hybridization for cranial neural crest-specific transcription factors across developmental time-course. The morphology of the presented developmental stage precludes obtaining a clear lateral view. White arrowheads mark the pre-oral gut. B, branchial NC stream; H, hyoid NC stream; H/B, hyobranchial sheet; Ma, mandibular NC stream; md, mandibular substream of mandibular NC stream; mx, maxillary substream of mandibular NC stream; optv, optic vesicle; otv, otic vesicle; r3, rhombomere 3; r5, rhombomere 5.

Fig. 5. *Expression summary of neural crest markers in CNC cells of the tropical gar from the specification through the late phase of migration.* (A-D) Micro-CT images showing dorsal views (A-D) of CNC developmental stages. (E-H) *Krox20* expression showing position of rhombomere 3 and 5. (I-T) Dorsal views of embryos after in situ hybridization for cranial neural crest-specific transcription factors across

developmental time-course. White arrowheads mark the pre-oral gut. B, branchial NC stream; H, hyoid NC stream; Ma, mandibular NC stream; r3, rhombomere 3; r5, rhombomere 5.

Fig. 6. *Expression summary of neural crest markers in CNC cells of the northern pike from the specification through the late phase of migration.* (A-D) DAPI staining showing dorsal views of CNC developmental stages. (E-H) *Krox20* expression showing position of rhombomere 3 and 5. (I-R) Dorsal views of embryos after in situ hybridization for cranial neural crest-specific transcription factors across developmental time-course. B, branchial NC stream; H, hyoid NC stream; Ma, mandibular NC stream; mxd, maxilo-mandibular subpopulation of mandibular NC stream; optv, optic vesicle; prp, pre-optic subpopulation of mandibular NC stream; r3, rhombomere 3; r5, rhombomere 5; rhom, rhombencephalon.

Fig. 7. *Comparison of SOX9 protein expression in CNC cells from the emigration through the late phase of migration*. Anti-SOX9 antibody visualizes individual neural crest cells of bichir (A-C), sterlet (D-F), gar (G-I), and pike (J-L). Dorsal (A, D-G, J) and lateral (B-C, H-I, K-L) views of cranial regions of examined embryos. White arrowheads mark the pre-oral gut and its derivatives. Asterisks mark exit points of mandibular substreams. B, branchial NC stream; e, eye primordium; H, hyoid NC stream; H/B, hyobranchial sheet; Ma, mandibular NC stream; optv, optic vesicle; otv, otic vesicle; pp1-2, pharyngeal pouch 1- 2; r3, rhombomere 3; r5, rhombomere 5; s0, somite 0.

Fig. 8. *Accelerated hyoid neural crest stream is associated with development of hyoid species-specific structures. Sox9* (A-C, F-G, K-M) and *Sox10* (H) expressions in CNC cells reveal accelerated emigration of the hyoid NC stream in bichir (A), gar (F), and pike (K). Dorsal (A-B, F-G, K-L) and lateral (C, H, M) views of cranial region of examined embryos. (D, I, N) *Hand2* expression reveals first CNC cells populating the pharyngeal region. Dorsal (D) and lateral (I, N) views of cranial region of examined embryos. (E, J, O) Accelerated development of the hyoid stream of NC cells is associated with morphogenesis of key hyoid structure like external gills of bichir (E), large opercular flap of gar (J), and

Journal Pre-proof

first forming cartilage in pike larvae (O). White arrowheads mark the pre-oral gut and its derivatives. B, branchial NC stream; e, eye primordium; exg, external gill; H, hyoid NC stream; hs, hyosymplectic; Ma, mandibular NC stream; op, opercular flap; otv, otic vesicle.

Fig. 9. *CM-DiI fate-mapping reveals contribution of hyobranchial sheet cells into hyoid and branchial streams in the sterlet sturgeon.* (A) Scheme of CM-DiI microinjection into mandibular (Ma) and hyobranchial (H/B) CNC exit points and contribution of each CNC subpopulation into the developing head. (B, F) Dorsal views of embryos at the time of injection. (C-E) Mandibular and hyobranchial (G-I) neural crest fate mapping (CM-DiI magenta). Superimposed fluorescent and dark-field images at successive stages of development. (C, D, G, H) Dorsal and lateral (E, I) views, anterior to the left. White arrowheads mark the pre-oral gut and its derivatives. B, branchial NC stream; H, hyoid NC stream; H/B, hyobranchial sheet; Ma, mandibular NC stream; mx + md, maxillo-mandibular subpopulation of mandibular NC stream; optv, optic vesicle; otv, otic vesicle; p1-3, pharyngeal pouch 1-3; IV., fourth brain cavity.

Fig. 10. *The separation of a single hyobranchial sheet in the sterlet sturgeon is associated with the formation of a second pharyngeal pouch.* (A, D) SOX9 protein expression in CNC cells of sterlet. Dashed lines indicate the plane of sections shown in panel C and F. (B, E) 3D reconstruction of pharyngeal endoderm (yellow). (C, F) Transverse section at the level of the hyobranchial sheet. Dotted lines mark the position of ectoderm (orange) and endoderm (yellow). White arrowheads mark the pre-oral gut. Asterisk marks a not well-developed second pharyngeal pouch. b, brain primordium; B, branchial NC stream; H, hyoid NC stream; H/B, hyobranchial sheet; Ma, mandibular NC stream; not, notochord; optv, optic vesicle; otv, vesicle; p1-2, pharyngeal pouch 1-2.

Fig. 11. *Ray-finned fishes reveal significant modification in the canonical pattern of CNC migration of vertebrates.* A cartoon of CNC migration and patterning (red) in representatives of all phylogenetic

lineages of ray-finned fishes (bichir - Cladistia, sterlet - Chondrostei, gar - Holostei, and pike - Teleosts) (red star), in typical model systems of lobe-finned fishes (chick and xenopus) (blue star) and in shark and lamprey as outgroups. Notice that emigration of the hyoid CNC stream (H) is remarkably accelerated in bichir, gar and pike and further that sterlet CNC cells constitute a single hyobranchial sheet. The top two lines demonstrate the dorsal view and the bottom line the lateral view. The shades of red in the first two lines represent the individual mandibular (Ma; light red), hyoid (H; intermediate red), and branchial (B; dark red) NC streams. Yellow indicates the pharyngeal endoderm and its derivative, pre-oral gut (yellow-grey stripes). Light and dark grey indicates optic and otic vesicles. The dotted square defines the examined fish species. The drawings are adapted from several published studies (Ballard et al., 1993; Kuratani and Horigome, 2000; Theveneau and Mayor, 2012; Martik et al., 2019)

Fig. S1. *Bichir mandibular CNC stream is separated into two substreams.* (A-B) *Sox9* expression in CNC cells of bichir. (A) Dorsal and lateral (B) views with indicated plane of transverse sections (dotted lines). (C-D) Transverse section at the level of individual mandibular substreams. Identical sections stained with DAPI are marked by ('). nf, neural fold; np, neural plate.

Fig. S2. *Identification of a single hyobranchial sheet of sterlet.* (A-D) Developmental stage at which a single hyobranchial sheet can be identified and (E-G) developmental stage after its separation. (A, E) microCT visualization showing analyzed developmental stages. Cyan indicates position of otic vesicle and green shows location of otic vesicle. (B, F) Left part shows SOX9 protein expression (red) and the right part demonstrate *Krox20* expression at the same level. (C, G) SOX9 protein expression in the embryo after in situ hybridization of *Krox20* revealing position of r3 and r5. (D) 'Double' in situ hybridization of *Sox9* and *Krox20* shows locations of hyobranchial sheet in the context of r3 and r5. All images represent dorsal views. White arrowheads mark the pre-oral gut. B, branchial NC stream; H, hyoid NC stream; H/B, hyobranchial sheet; Ma, mandibular NC stream; optv, optic vesicle; otv, otic vesicle; r3, rhombomere 3; r5, rhombomere 5.

Journal Pre-proof

Fig. S3. *Hyoid pharyngeal endoderm expands laterally and contributes to the formation of gar opercular flap.* (A-D, F-I, K-N, P-S) 3D reconstruction of pharyngeal endoderm (yellow), optic vesicle (cyan) and otic vesicle (green). (A, F, K, P) Dorsal and (C, H, M, R) lateral views on volume rendering of the analyzed embryo. (B, G, L, Q) Dorsal and (D, I, N, S) lateral views on 3D rendered model of reconstructed areas. (E, J, O, T) Transverse section shows a lateral expansion of the hyoid pharyngeal endoderm (white arrow). White arrowheads mark the pre-oral gut and its derivatives. Black arrowheads mark the hyoid pharyngeal endoderm. op, opercular flap; optv, optic vesicle (cyan); ot, otic vesicle (green).

Journal Pre-proof

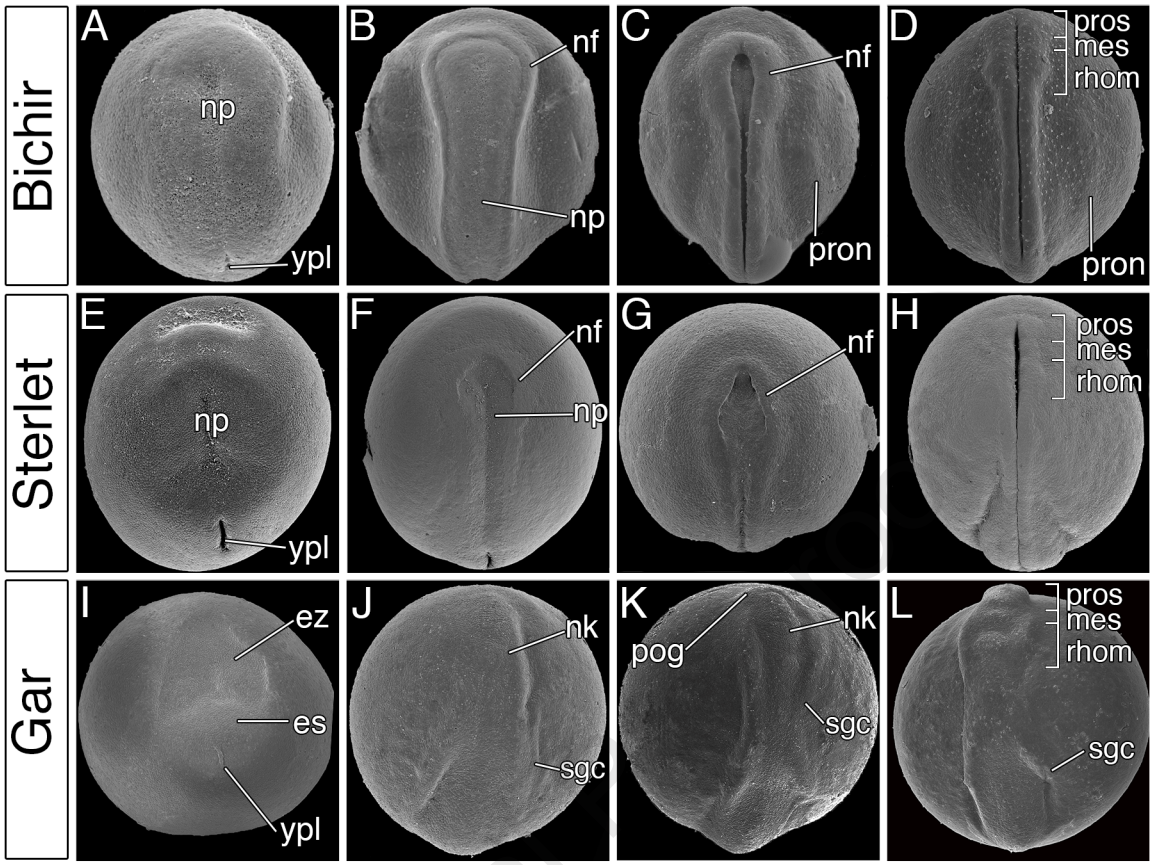
Bichir
Sterlet
Gar
A
np
ypl
B
nf
np
C
nf
pron
D
pros
mes
rhom
pron
E
np
ypl
F
nf
np
G
nf
H
pros
mes
rhom
I
ez
es
ypl
J
nk
sgc
K
pog
nk
sgc
L
pros
mes
rhom
sgc

Journal

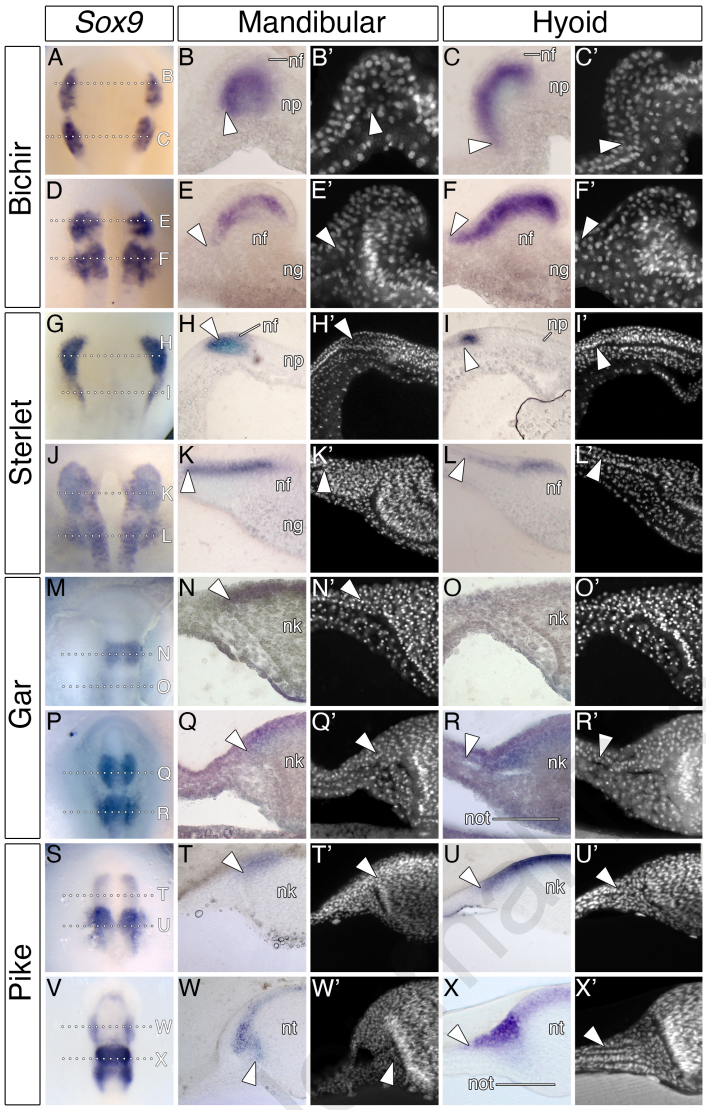

Journal Pre-proof

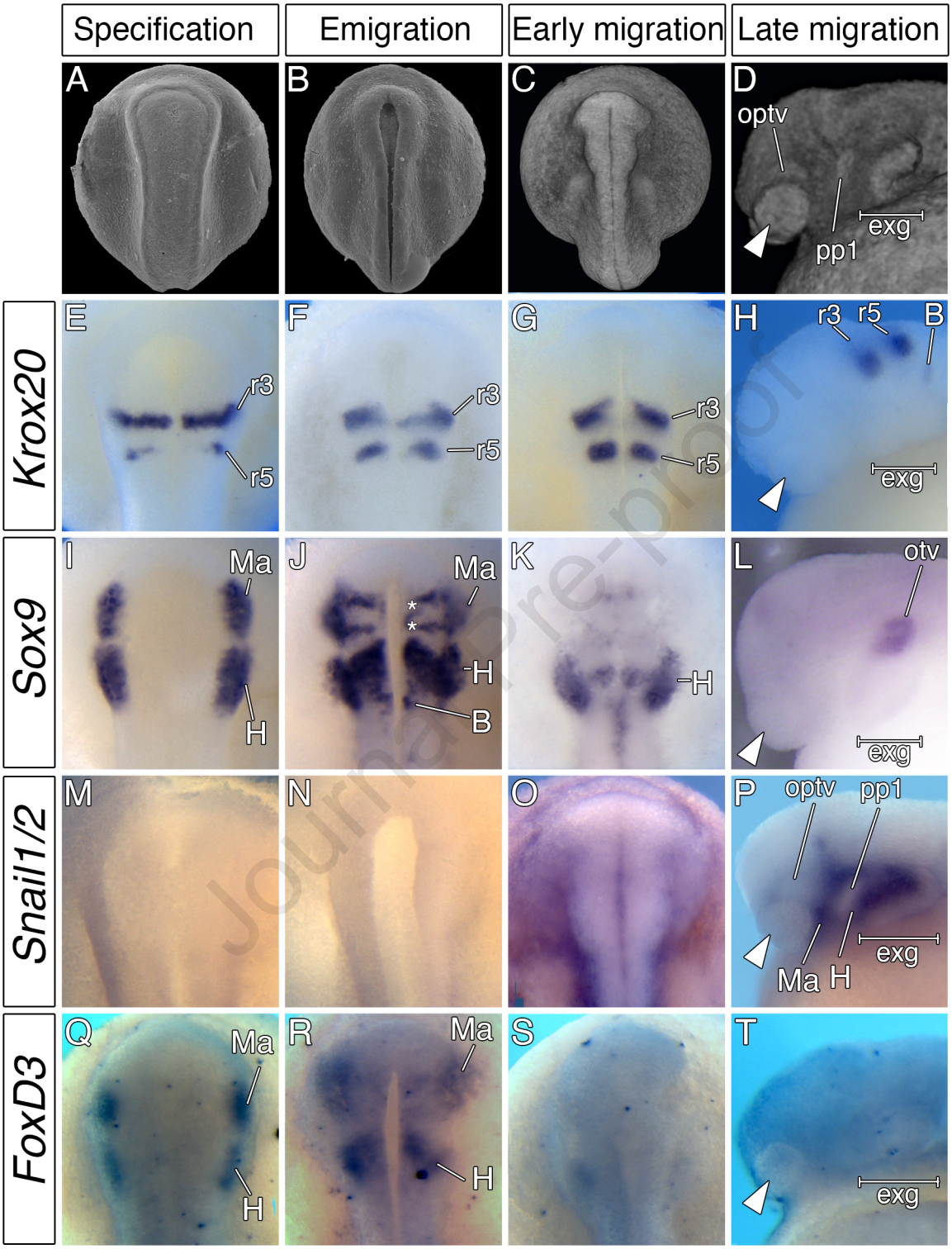

Journal Pre-proof

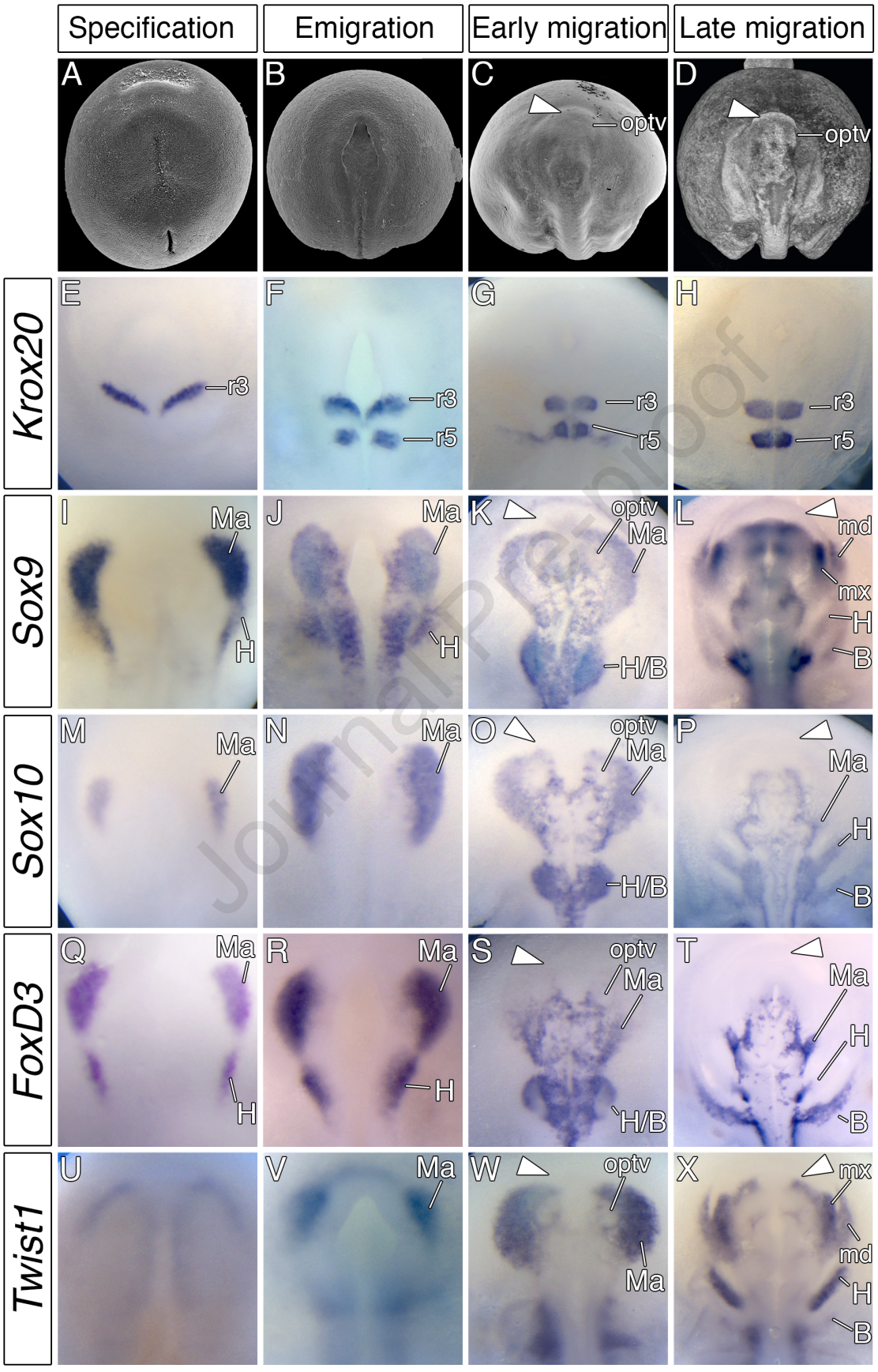

Journal Pre-proof

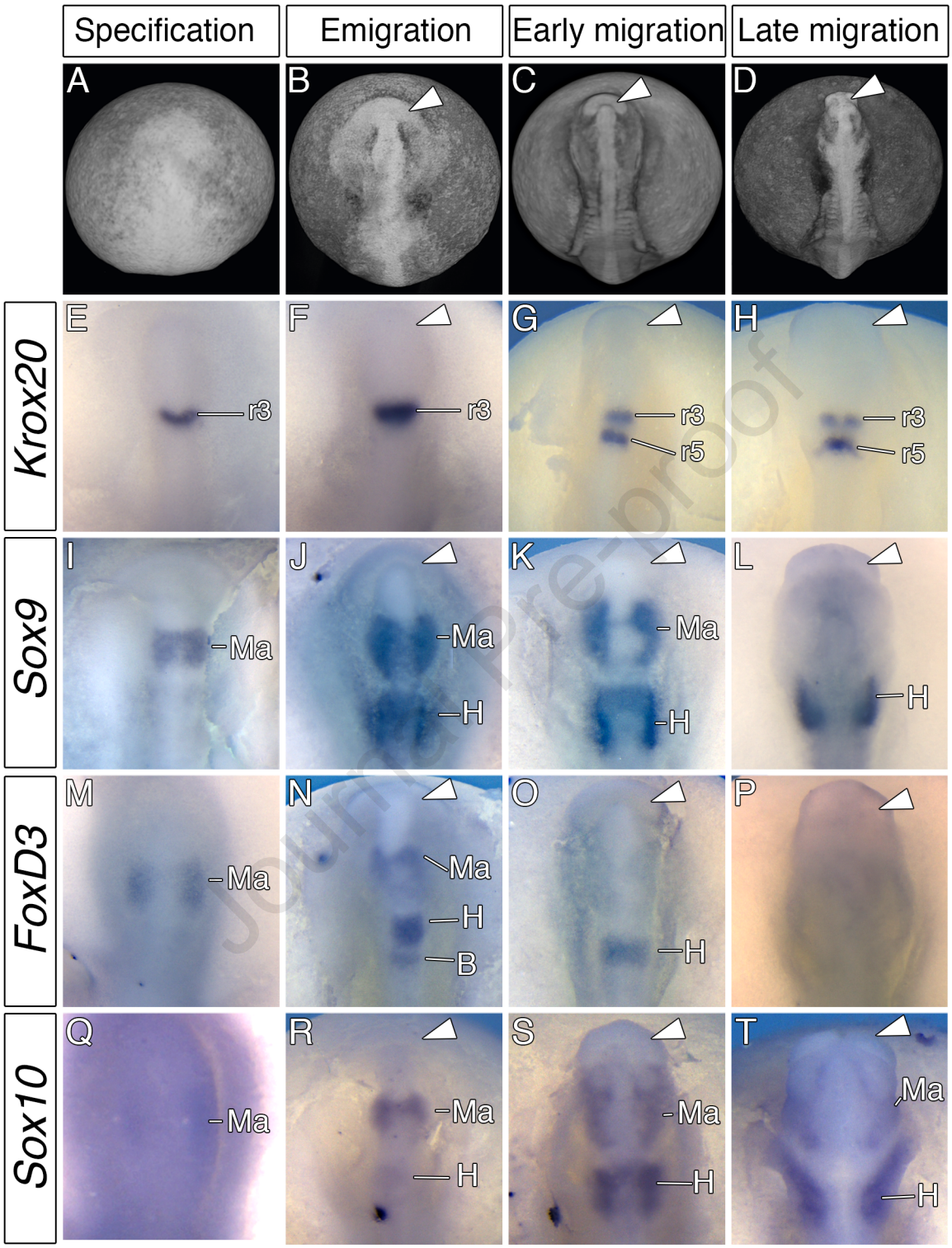

Journal Pre-proof

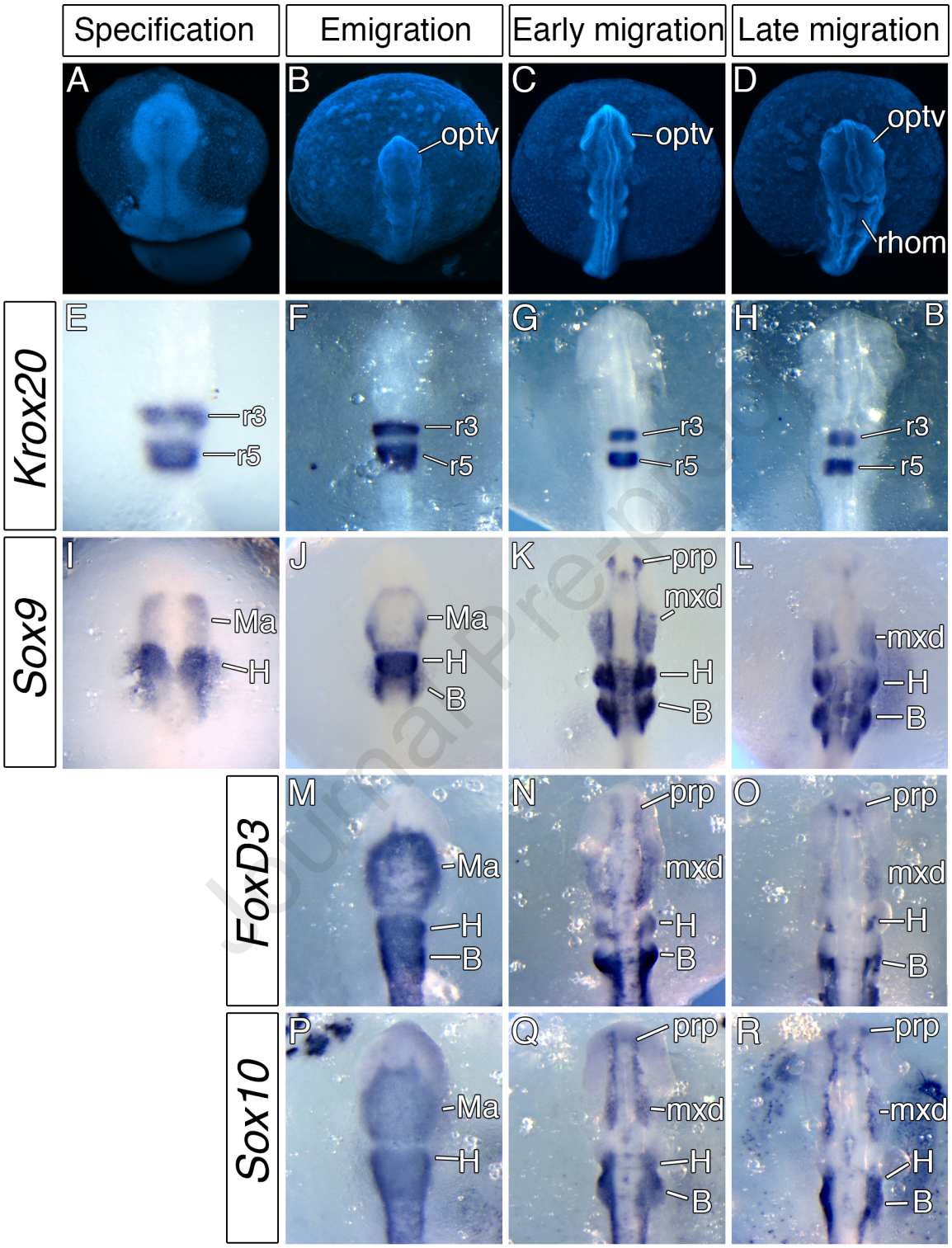

Journal Pre-proof

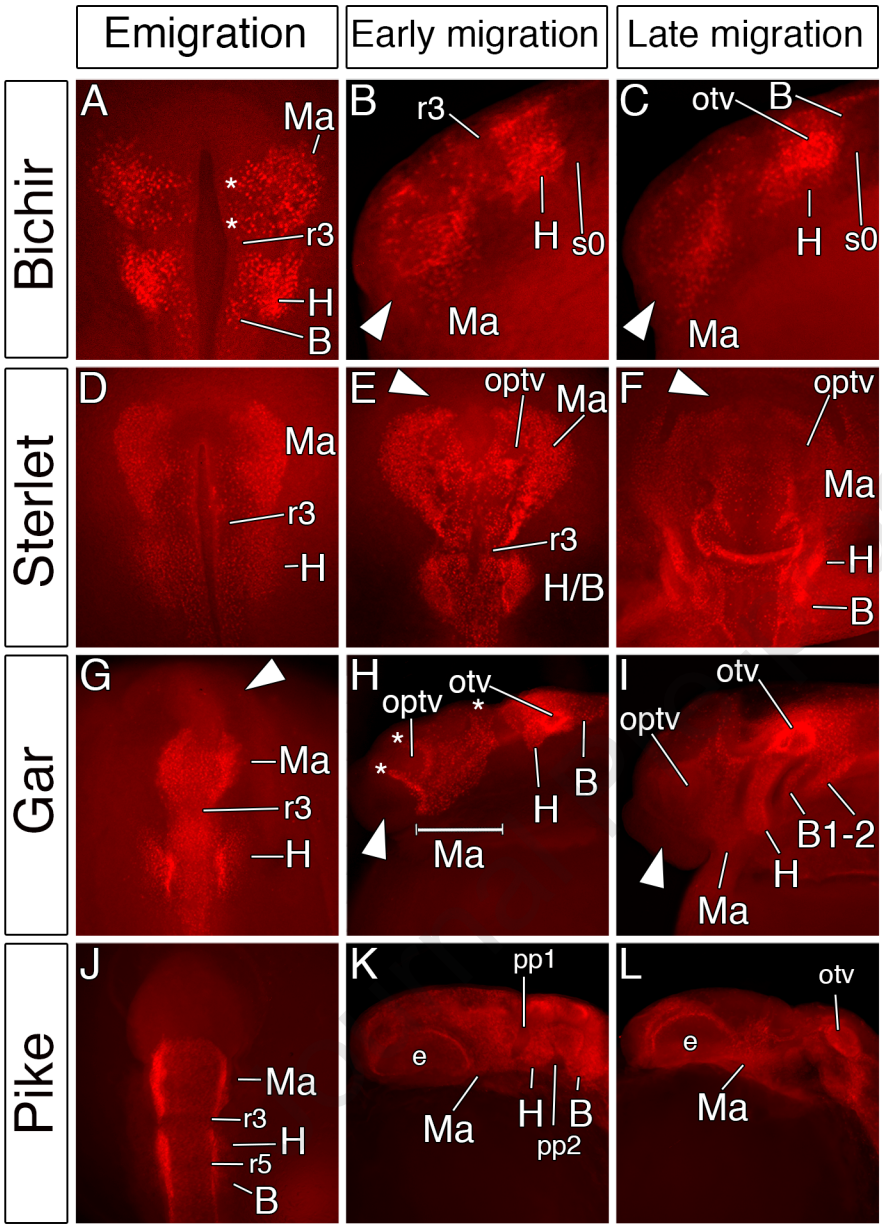
Emigration
Early migration
Late migration
Bichir
Sterlet
Gar
Pike
A
Ma
r3
H
B
B
r3
H
s0
Ma
C
otv
B
H
s0
Ma
D
Ma
r3
H
E
optv
Ma
r3
H/B
F
optv
Ma
H
B
G
Ma
r3
H
H
optv
otv
H
B
Ma
I
otv
optv
B1-2
H
Ma
J
Ma
r3
H
r5
B
K
pp1
e
Ma
H
B
pp2
L
otv
e
Ma

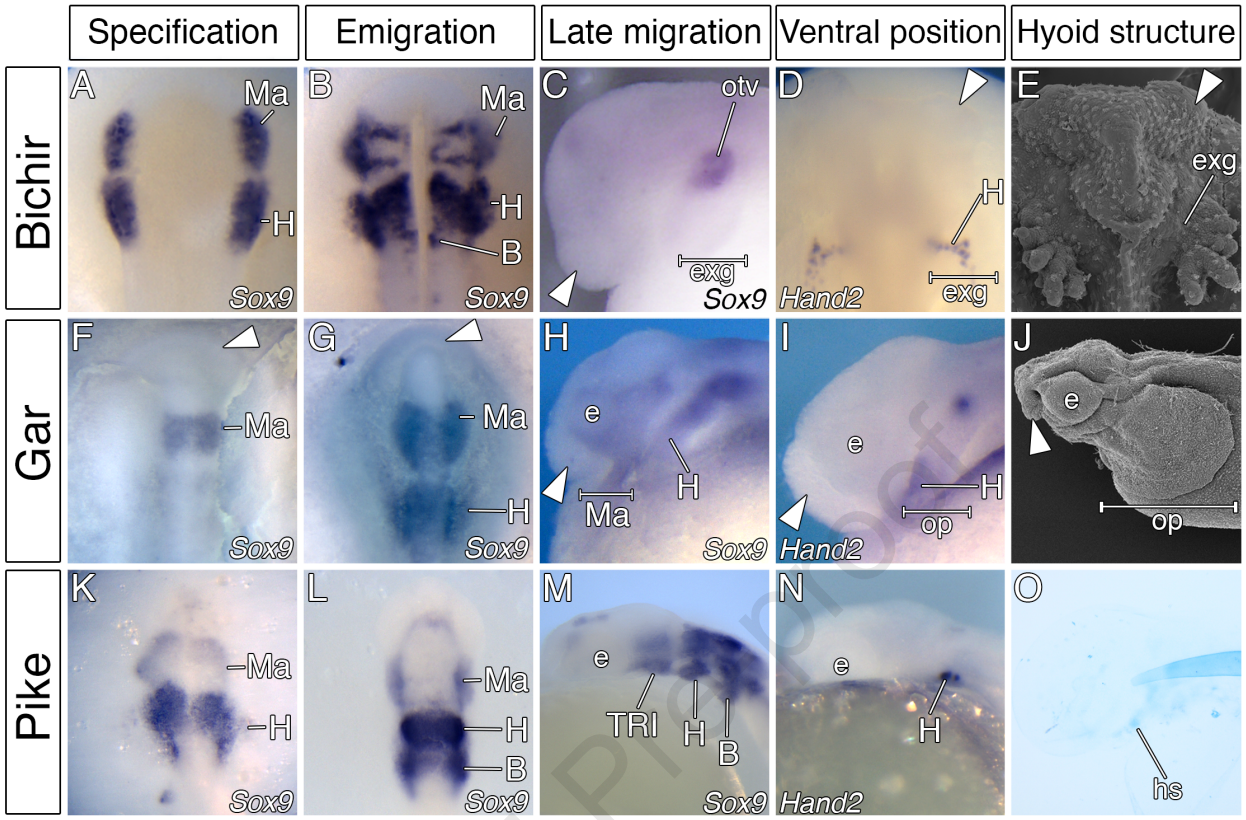

Journal Pre-proof

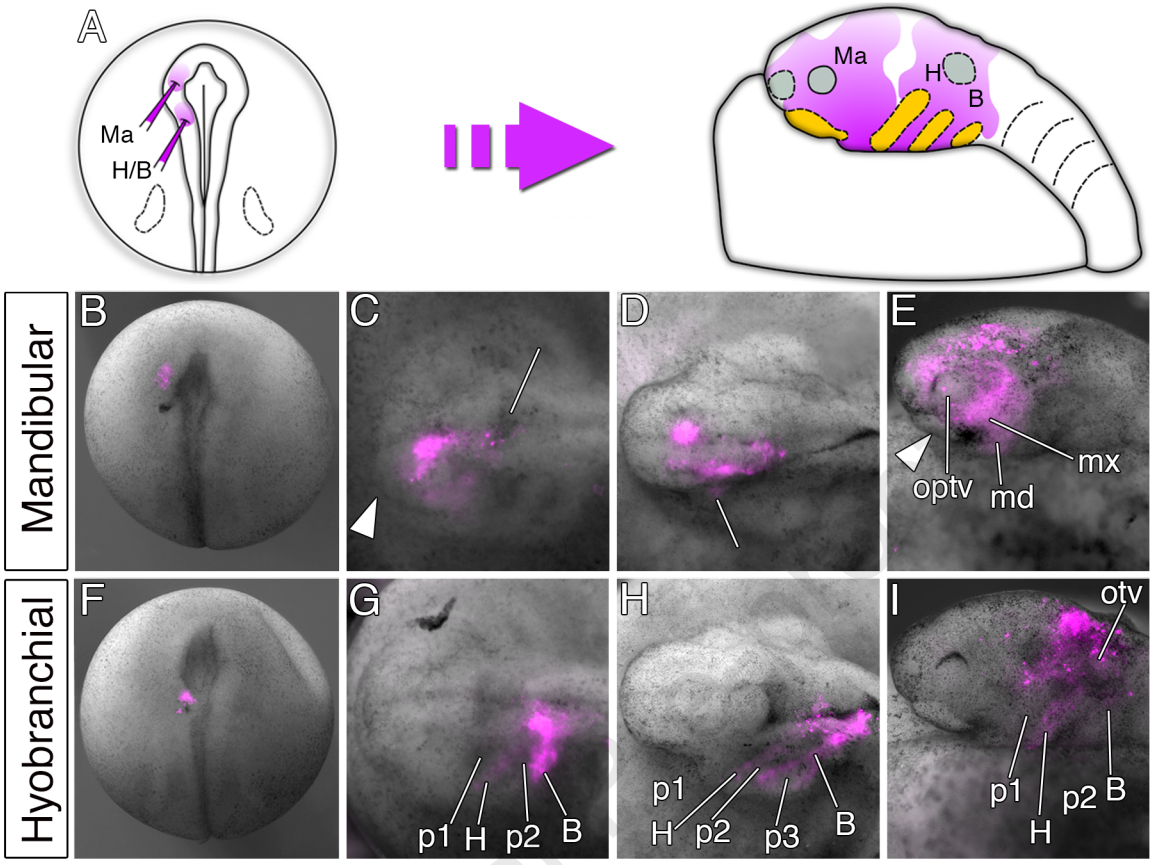

Journal Pre-proof

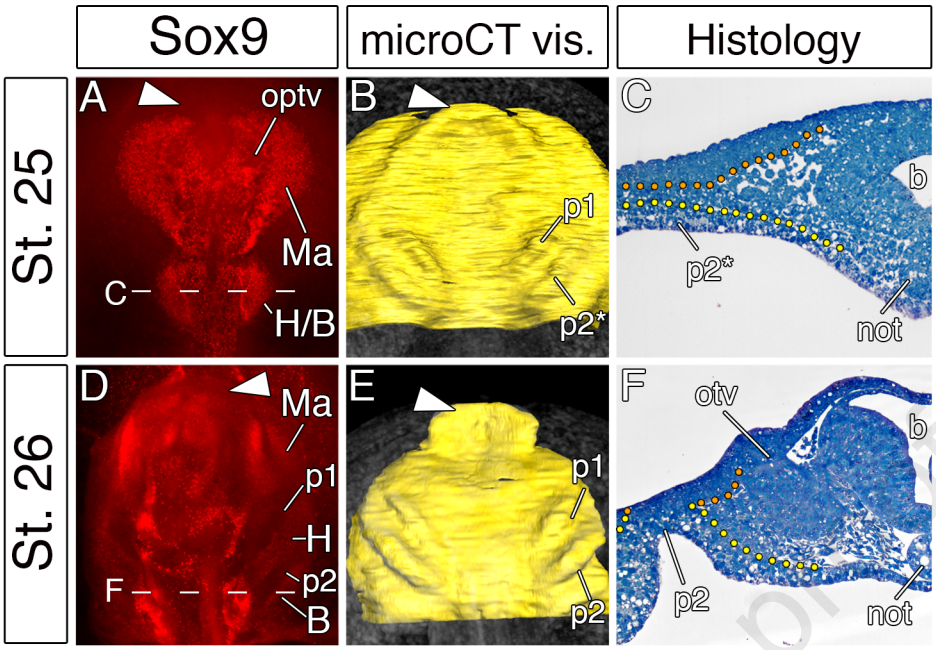

Journal Pre-proof

Journal Pre-proof

Highlights:

- First comprehensive analysis of cranial neural crest migration in ray-finned fishes
- Unique cranial neural crest migratory patterns among vertebrates
- Heterochronies in neural crest migratory patterns influences craniofacial diversity

Journal Pre-proof